

HOSTED BY



ELSEVIER

Contents lists available at ScienceDirect

China University of Geosciences (Beijing)

Geoscience Frontiers

journal homepage: [www.elsevier.com/locate/gsf](http://www.elsevier.com/locate/gsf)

## Research Paper

## São Francisco–Congo Craton break-up delimited by U–Pb–Hf isotopes and trace-elements of zircon from metasediments of the Araçuaí Belt

Mathias Schannor\*, Cristiano Lana, Marco A. Fonseca

Applied Isotope Research Group, Department of Geology, Universidade Federal de Ouro Preto, Morro do Cruzeiro, Ouro Preto, 35400-000, MG, Brazil

## ARTICLE INFO

## Article history:

Received 25 August 2017

Received in revised form

4 January 2018

Accepted 7 February 2018

Available online xxx

Handling Editor: Wen-jiao Xiao

## Keywords:

Detrital zircon

U–Pb geochronology

Lu–Hf isotopes

Trace elements

Araçuaí Belt

## ABSTRACT

Detrital zircon U–Pb geochronology combined with Hf isotopic and trace element data from meta-sedimentary rocks of the Araçuaí Belt in southeastern Brazil provide evidence for break-up of the Congo–São Francisco Craton. The U–Pb age spectra of detrital zircons from metasediments of the Rio Doce Group (RDG) range from 900–650 Ma and define a maximum depositional age of ca. 650 Ma. Zircon trace element and whole rock data constrain an oceanic island arc as source for the deposition setting of the protoliths to the metasediments. Zircon  $\varepsilon_{\text{Hf}}(t)$  values from these rocks are positive between +1 and +15, supporting previous evidence of a Neoproterozoic extensional phase and oceanic crust formation in a precursor basin to the Araçuaí Belt. Recrystallization of detrital zircon at ca. 630 Ma is compatible with a regional metamorphic event associated with terrane accretion to the Paleoproterozoic basement after transition from an extensional to a convergent regime. The juvenile nature, age spectra and trace element composition recorded in detrital zircons of metasediments from the Araçuaí Belt correspond with zircons from metasedimentary rocks and oceanic crust remnants of other orogenic belts to its south. This suggests that rifting and oceanic crust formation of the entire orogenic system, the so-called Mantiqueira Province, was contemporaneous, most likely related to the opening of a large ocean. It further indicates that the cratonic blocks involved in the orogenic evolution of the Mantiqueira Province were spatially connected as early as 900 Ma.

© 2018, China University of Geosciences (Beijing) and Peking University. Production and hosting by Elsevier B.V. This is an open access article under the CC BY-NC-ND license (<http://creativecommons.org/licenses/by-nc-nd/4.0/>).

## 1. Introduction

The Neoproterozoic break-up of the Rodinia supercontinent and assembly of Gondwana is one of the most important events concerning geodynamics, palaeoclimatic changes, and development of biologic diversity on Earth (Hoffman et al., 1998; Meert and Liebermann, 2008; Nance et al., 2014). In palaeogeographic reconstructions, the Amazonian Craton is usually considered part of Rodinia whereas the Río de la Plata, Kalahari and São Francisco–Congo Cratons were marginal to Rodinia (e.g. D'Agrella-Filho and Cordani, 2017; Oriolo et al., 2017). However, South American and African Cratons were possibly positioned within the Rodinia supercontinent (Evans, 2009). The assembly of Rodinia during the Grenvillian Orogeny was a long-lasting process (1.45–0.97 Ga) whereas its break-up appears synchronous at ca.

750 Ma (e.g. Li et al., 2008; Evans, 2009; D'Agrella-Filho and Cordani, 2017). Contrastingly, rifting and collisional events of South American and African continental masses were diachronic processes between 1.00–0.75 Ga (D'Agrella-Filho and Cordani, 2017). Later accretion of West Gondwana (combined Africa and South America; Fig. 1a) connected several continental blocks in a network of orogens to build a crustal mosaic in the Ediacaran and early Cambrian from 640–520 Ma (Trompette, 1997; Brito Neves et al., 1999; Alkmim et al., 2006; Fig. 1a). Neoproterozoic collisional belts are better known, whereas little is known about timing of rifting and break-up in South American continental blocks.

The Mantiqueira Province is a section of this large orogenic system extending alongside the southeastern coast of Brazil and Uruguay (e.g. Almeida et al., 1981; Silva et al., 2005; Fig. 1a). The co-evolution of the orogenic belts of the Mantiqueira Province remains a matter of debate, in spite of detailed description of each composing belt (e.g. Silva et al., 2005; Bento dos Santos et al., 2015). Contradiction exists between models that favour multiple collisions of different microplates over a single diachronic collisional event in the orogenic province (e.g. Heilbron and Machado, 2003; Bento dos

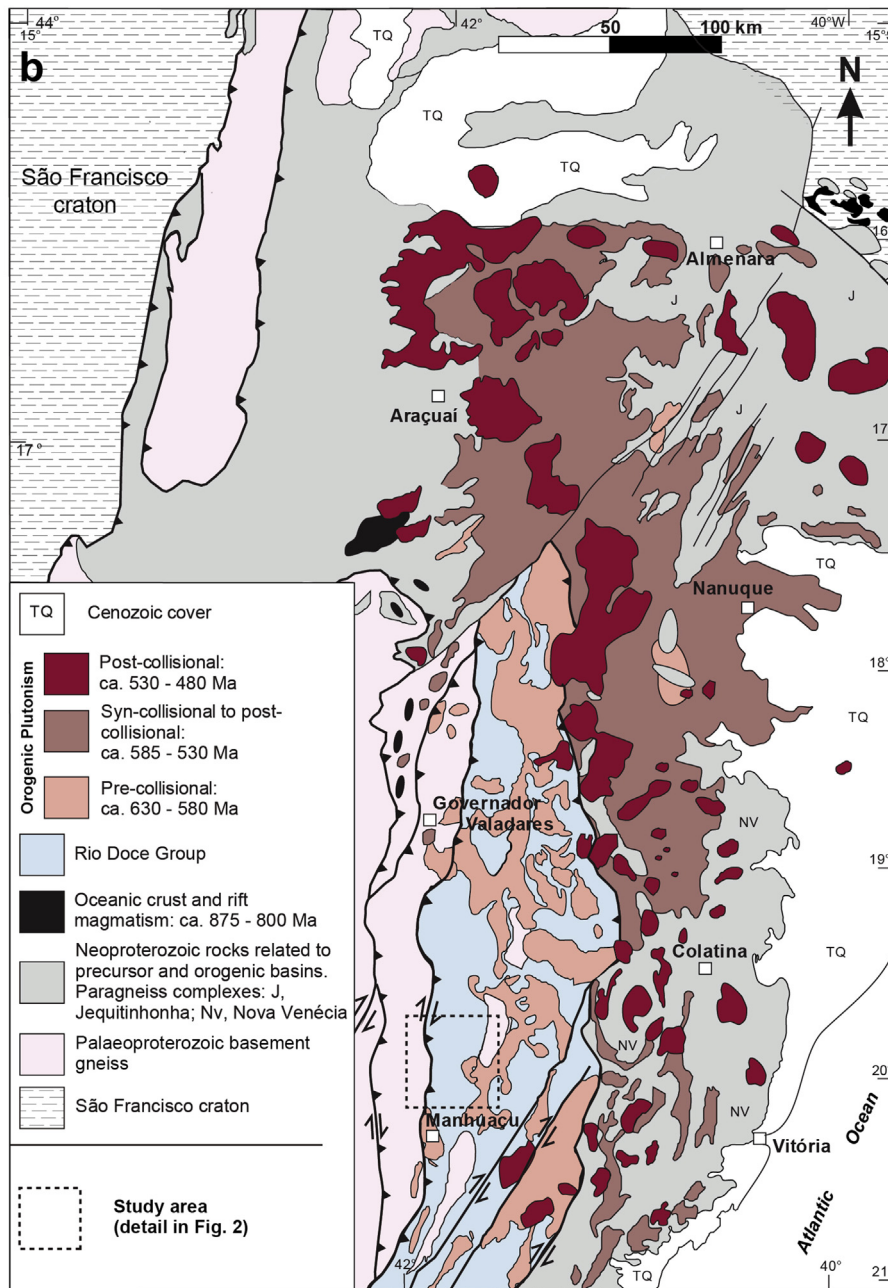
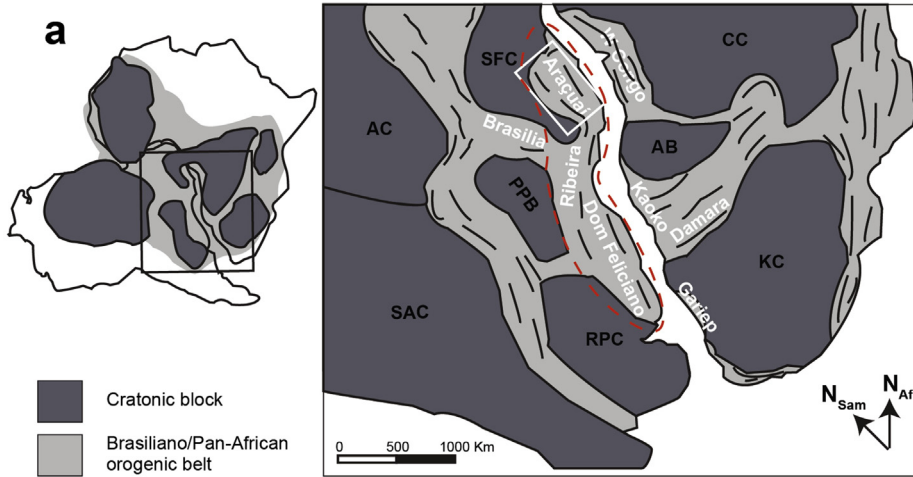
\* Corresponding author.

E-mail address: [m.schannor@gmail.com](mailto:m.schannor@gmail.com) (M. Schannor).

Peer-review under responsibility of China University of Geosciences (Beijing).

<https://doi.org/10.1016/j.gsf.2018.02.011>

1674-9871/© 2018, China University of Geosciences (Beijing) and Peking University. Production and hosting by Elsevier B.V. This is an open access article under the CC BY-NC-ND license (<http://creativecommons.org/licenses/by-nc-nd/4.0/>).



Santos et al., 2015). It is noteworthy however, that these models mostly hinge on studies of orogenic magmatism; the lack of provenance studies in this area weakens all tectonic models. This limitation of studies restrains large-scale palaeo-reconstructions of Gondwana assembly where rifting during Rodinia break-up at ca. 750 Ma and later amalgamation of continental blocks are evident. As a consequence, many aspects of the geodynamic history are still debated (e.g. Li et al., 2008; Frimmel et al., 2011; Evans et al., 2016).

Paleogeographical reconstructions of orogenic belts are strengthened with the integrated use of provenance of sedimentary rocks and palaeomagnetic and event chronology (e.g. Anderson, 2005; Cawood et al., 2007). Detrital zircon is increasingly used for provenance analysis in geodynamic evolution and paleogeographical modelling (e.g. Cawood et al., 2007; Gehrels, 2014). Zircon ages help to constrain the timing of deposition of sediments, reconstruction of provenance by matching the age with known zircon-forming events, and basin modelling as a sink of zircon (e.g. Cawood et al., 2012; Gehrels, 2014). Combining zircon detrital ages and Hf isotopic compositions overcomes limitations of this method such as lack of outcrop or erosion of certain source rock units, or multiple potential source areas with similar zircon crystallization ages (e.g. Augustsson et al., 2006; Howard et al., 2009). This approach is increasingly used to identify different source areas with similar ages because the Hf isotopic signature of individual zircons is revealing the juvenile and crustally evolved contribution of the source region.

In this contribution we investigate the provenance of meta-sedimentary rocks of the Rio Doce Group (RDG) from the Araçuaí Belt in southeastern Brazil, in the northern sector of the Mantiqueira Province in order to improve our understanding of Gondwana assembly. We show results of zircon U–Pb–Hf isotopic and trace element analyses in comparison with previously published age spectra and isotopic compositions of zircon from potential source areas in West Gondwana and other metasedimentary units of the Mantiqueira Province. Based on this approach, we present new constraints on the depositional age, provenance and tectonic setting of the protoliths to the studied metasediments, with implications for the geodynamic evolution of West Gondwana.

## 2. Geological setting

### 2.1. The Mantiqueira Province

The Mantiqueira Province is a geographical division of the Brasileiro Orogen, extending for ~3000 km alongside the Atlantic coast of southeastern Brazil and Uruguay. The orogen has the Pan-African Orogen as a counterpart and comprises, from south to north, the Dom Feliciano Belt (DFB), Ribeira Belt (RB) and Araçuaí Belt (AB or Araçuaí Orogen) in South America and the West-Congo, Kaoko, Damara and Gariep Belts in Africa (Almeida et al., 1981; Da Silva et al., 2005; Bento dos Santos et al., 2015; Fig. 1a). These orogenic belts connect a mosaic of Archean and Palaeoproterozoic basement blocks and Meso- and Neoproterozoic sedimentary basins that were amalgamated during closure of the Adamastor and the Khomas Oceans (e.g. Brito-Neves and Cordani, 1991; Pedrosa-Soares et al., 2001; Silva et al., 2005). Subsequent rifting of the South Atlantic in the Cretaceous separated the South American from the African belts. The orogenic systems are limited to the west by the São Francisco, Paranapanema and Rio de la Plata Cratons and to the east by the Congo and Kalahari Cratons (Fig. 1a).

Rift-related volcanics and anorogenic granites (ca. 900 Ma, Machado et al., 1989; da Silva et al., 2008) together with inferred ophiolite remnants in the AB (ca. 800 Ma, Pedrosa-Soares et al., 1998) provide evidence for a Neoproterozoic ocean in the northern Mantiqueira Province. Extensional magmatism in the RB (ca. 800–770 Ma, Heilbron and Machado, 2003) and ophiolitic remnants in the DFB (ca. 900 Ma and 750 Ma, Saalman et al., 2005; Arena et al., 2016) are evidence of a southern continuation of that ocean. Closure of this ocean gave rise to magmatic arc development in the three belts at ca. 630–570 Ma (e.g. Pedrosa-Soares et al., 2001; Heilbron and Machado, 2003; da Silva et al., 2005; Saalman et al., 2005). Subsequent collision resulted in production of syn-orogenic granites at ca. 590–570 Ma with associated granulite-facies metamorphism and anatexis in the DFB and AB (Leite et al., 2000; Pedrosa-Soares et al., 2001; da Silva et al., 2005; Richter et al., 2016; Melo et al., 2017). Final pulses of magmatism from 530 Ma to 480 Ma mark the terminal amalgamation of continental blocks (Pedrosa-Soares et al., 2001; da Silva et al., 2005; Richter et al., 2016). Compared to the AB and RB, an initial phase of juvenile magmatism at ca. 850 Ma was followed by continental arc magmatism in the DFB between 770 Ma and 680 Ma (São Gabriel Block, e.g. Babinski et al., 1996; Saalman et al., 2005; Lena et al., 2014). The main collisional event occurred between 650 Ma and 580 Ma with subsequent anatexis and production of large granitic bodies (e.g. Saalman et al., 2005; Bento dos Santos et al., 2015).

The geodynamic evolution of the Mantiqueira Province remains debated. Many authors suggest a diachronic single collisional event (da Silva et al., 2005; Bento dos Santos et al., 2015), whereas others argue for multiple collisions of several microplates (Campos Neto and Figueiredo, 1995; Heilbron and Machado, 2003). Bento dos Santos et al. (2015) compiled geochronological and geochemical data for the entire Mantiqueira Province and proposed a single collisional event based on similar chemical signatures of magmatic rocks in different periods in all belts with progressively younger ages towards the northern section of the entire orogenic system. Heilbron and Machado (2003) reported a metamorphic event (540–520 Ma) only present in some terranes of the RB, and proposed a scenario of several collisional events between microplates containing the main cratonic blocks.

### 2.2. The Araçuaí Belt

The Araçuaí Belt in southeastern Brazil and its African counterpart, the West-Congo Belt, developed between the São Francisco and Congo Cratons and represent the northern end of the Mantiqueira Province (e.g. Pedrosa-Soares et al., 2001; Alkmim et al., 2006; Fig. 1a). The West-Congo Belt only hosts one third of the combined Brasileiro/Pan-African system and consists mainly of low-grade metamorphic rift to proximal passive margin sequences of the precursor basin and no orogenic magmatic rocks (Tack et al., 2001). The Araçuaí Belt, representing two thirds of the system, constitutes rift-related to distal passive margin sequences of the precursor basin, a continental magmatic arc, and collisional- and post-collisional magmatic bodies (Pedrosa-Soares et al., 2001, 2011; Alkmim et al., 2006; Fig. 1b). The basement in the western portion of the Araçuaí Belt includes Archean gneisses of the São Francisco Craton, greenstone belt remnants and Palaeoproterozoic supra-crustal lithologies that were affected by the ~2.00 Ga Transamazonian Orogeny and later on reworked during the Brasileiro

**Figure 1.** (a) Position of cratonic blocks and Neoproterozoic orogenic belts of southwestern Gondwana. The dashed line delineates the extent of the Mantiqueira Province. Abbreviations: AB – Angola Block, AC – Amazonian Craton, CC – Congo Craton, KC – Kalahari Craton, PPB – Paranapanema Block, RPC – Rio de la Plata Craton, SAC – South America Megacraton, SFC – São Francisco Craton (modified from Frimmel et al., 2011; Rapela et al., 2011). (b) Geological map of the Araçuaí Belt (modified from Pedrosa-Soares et al., 2001; Melo et al., 2017).

Orogeny (e.g. Alkmim and Marshak, 1998; Pedrosa-Soares et al., 2001). Archean–Palaeoproterozoic basement units in the central Araçuaí Belt are made up of high-grade amphibolite-to granulite-facies rocks represented by the Juiz de Fora and Pocrane Complexes (Pedrosa-Soares et al., 2001; Gonçalves et al., 2014). According to their isotopic signature, these 2.20 to 2.00 Ga old gneissic units are interpreted as juvenile magmatic arcs sutured with the São Francisco Craton during the Transamazonian Orogeny (e.g., Alkmim and Marshak, 1998; Pedrosa-Soares et al., 2001; Gonçalves et al., 2014). A major rifting phase occurred at ca. 1.75 Ga, represented by the Espinhaço Supergroup which is found in the external fold-thrust belt on the western margin of the Araçuaí Belt (Alkmim et al., 2006; Chemale et al., 2012). The Macaúbas Group represents the precursor basin of the Araçuaí Belt and records a first rifting phase during the Neoproterozoic between 1000 Ma and 850 Ma (Pedrosa-Soares et al., 2001; Alkmim et al., 2006; Babinski et al., 2012; Kuchenbecker et al., 2015). Proximal tillite, diamictite, sandstone and pelite deposits of the Macaúbas Group provide evidence of an 850 Ma old glaciation event (e.g., Alkmim et al., 2006; Babinski et al., 2012). Some distal metamorphosed mafic to ultramafic rocks of this basin are interpreted as oceanic crust remnants. Amphibolites of this assemblage have been dated at 820 Ma with a juvenile Nd isotopic signature and are described as oceanic crust of the rifting event (Pedrosa-Soares et al., 1998).

The crystalline core of the Araçuaí Belt constitutes voluminous orogenic igneous bodies that record the different stages of continent-continent convergence. The Rio Doce Arc has the pre-collisional magmatism of metaluminous granites from 630 Ma to ca. 580 Ma (e.g., Pedrosa-Soares et al., 2011; Gonçalves et al., 2014, 2015). During the syn-collisional stage large peraluminous batholiths intruded between 585 Ma and 560 Ma (e.g., Pedrosa-Soares et al., 2011; Richter et al., 2016; Melo et al., 2017). Subsequently late-to post-collisional peraluminous leucogranites were emplaced from 545 Ma to 530 Ma (Pedrosa-Soares et al., 2001, 2011). In response to gravitational collapse in the post-collisional stage, a final suite of granitic to noritic plutons intruded the internal zone of the Araçuaí Belt between 530 Ma and 480 Ma (Pedrosa-Soares et al., 2001, 2011; Alkmim et al., 2006; Richter et al., 2016). Granulite-facies anatectic paragneiss complexes Jequitinhonha and Nova Venécia are found to the east of the crystalline core of the Araçuaí Belt and possibly represent metamorphosed passive margin or back-arc basins (Alkmim et al., 2006; Richter et al., 2016). The Rio Doce Group (RDG) that covers vast areas of the Paleoproterozoic basement in the western Araçuaí Belt is a little studied supracrustal unit (Figs. 1b and 2). The group consists of pelitic schist, quartzite, paragneiss and metagreywacke that were intruded by pre-collisional granitoids (Vieira, 2007; Gonçalves et al., 2015). The RDG also hosts metavolcanic sills of dacitic and rhyolitic compositions dated at ca. 585 Ma (Vieira, 2007; Gonçalves et al., 2014). The maximum depositional age of the metasediments was estimated at ca. 590 Ma (Vieira, 2007). Combined with field observations, the ages led some others to propose that the RDG metasediments are continental arc-related basin deposits and that the metavolcanic rocks are equivalent to the pre-collisional magmatism (Vieira, 2007; Pedrosa-Soares et al., 2011; Gonçalves et al., 2014). Metasedimentary rocks of the RDG are the focus of the present work.

### 3. Sampling

In the study area a transcurrent fault separates the RDG from the Palaeoproterozoic Pocrane Gneiss Complex (Fig. 2). Granite bodies of various sizes intruded the RDG during pre-collisional

magmatism (Fig. 2). According to Vieira (2007) the RDG can be divided in four sub-units, stratigraphically from bottom to top: (1) schists and paragneisses with lenses of amphibolite, calcsilicate rock and quartzite; (2) metavolcanic rocks; (3) garnet-staurolite schist; and (4) quartzite. All four RDG samples of this study were collected from the bottom sub-unit. Tuller (2000) described the occurrence of the RDG rocks in the study area as schists and paragneisses with amphibolite lenses and calcsilicate rocks.

#### 3.1. Outcrop POC3

Outcrop POC3 exposes as weakly foliated gneiss that contains amphibolite lenses. Sample POC3A was collected from an amphibolite lens. It is a medium-grained garnet-bearing amphibolite with hornblende (40%), quartz (30%), plagioclase (20%), biotite (5%) and garnet (5%). Accessory phases are muscovite, zircon, epidote and ilmenite. Hornblende-rich layers alternating with felsic quartz-plagioclase layers build the foliation. Sample POC3B is fine-grained garnet-quartz gneiss. The mineral assemblage includes quartz (40%), plagioclase (35%), biotite (15%), garnet (10%) and accessory zircon and ilmenite.

#### 3.2. Outcrop POC28

Outcrop POC28 consists of a banded gneiss intruded by pre-collisional granites (Fig. 2). Sample POC28A is biotite-quartz gneiss with a mineral assemblage of biotite (30%), quartz (25%), plagioclase (25%), epidote (10%) and garnet (10%). Accessory phases are chlorite, zircon, titanite and ilmenite. POC28B was collected from a granitic vein consisting of a quartz-plagioclase-biotite-epidote-garnet association with accessory zircon and titanite.

## 4. Analytical methods

### 4.1. Zircon U–Pb dating

Zircon grains were handpicked from heavy mineral separates of crushed and panned metasediment samples. Subsequently the grains were mounted in 25 mm-diameter circular epoxy mounts and polished to expose their cores. Prior to analysis, zircons were imaged by Scanning Electron Microscopy (SEM) using a JEOL 6510 equipped with a Centaurus cathodoluminescence (CL) detector at the Geoscience Department of the Universidade Federal de Ouro Preto (UFOP) (Brazil), to obtain information on their internal structures. Zircon U–Pb isotope analyses were performed by LA-ICPMS at UFOP using a Thermo-Fisher Element II sector field ICP-MS coupled to a CETAC LSX-213 G2 ( $\lambda = 213$  nm) Nd:YAG laser. A detailed description of the method is given by Gerdes and Zeh (2006, 2009). Ablation was carried out in a low-volume cell with helium as carrier gas; laser beam parameters used were a spot size of 20  $\mu\text{m}$ , a repetition rate of 10 Hz, and a fluence of  $\sim 3$  J  $\text{cm}^{-2}$ . Time-resolved raw data were corrected offline for background signal, common Pb, laser-induced elemental fractionation, instrumental mass discrimination, and time-dependent elemental fractionation of Pb/U using the GLITTER<sup>®</sup> software package (Van Achterbergh et al., 2001). Common Pb correction was applied using the interference- and background-corrected <sup>204</sup>Pb signal and a model Pb composition (Stacey and Kramers, 1975). Laser induced elemental fractionation and instrumental mass discrimination were corrected by normalization to the reference zircon GJ-1 (Jackson et al., 2004), which was routinely measured within each analytical session. The drift in inter-elemental fractionation (Pb/U) during 30s of sample ablation was corrected individually before

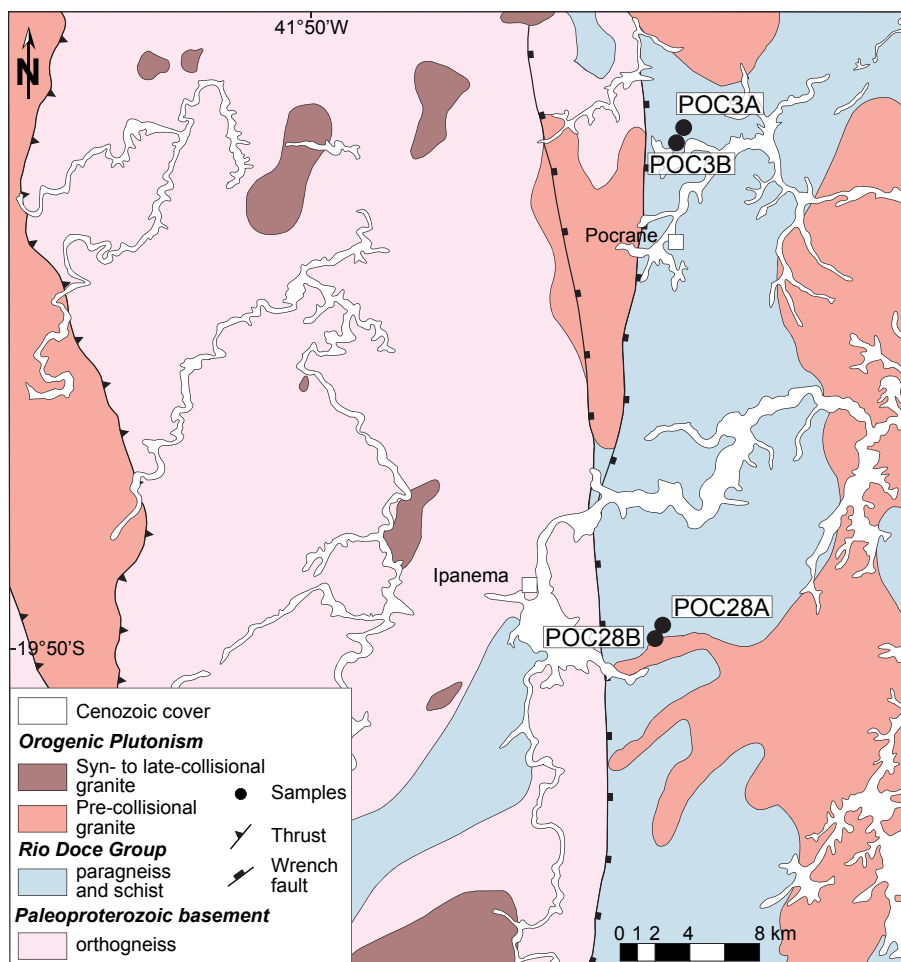


Figure 2. Simplified geological map of the study area with sample locations (modified from Tuller, 2000).

normalization to GJ-1. Reported uncertainties ( $2\sigma$ ) were propagated by quadratic addition of the external reproducibility obtained from the standard zircon GJ-1 during the analytical session (2SD in %) and the within-run precision of each analysis (standard error in %). In order to test the validity of the applied methods and the reproducibility of the data, multiple analyses of the reference zircon Plešovice (Sláma et al., 2008) were performed. Plešovice gave a concordia age of  $337 \pm 1$  Ma ( $n = 86$ , MSWD = 0.21). This is in agreement, within uncertainty, with the accepted ID-TIMS age reported for Plešovice ( $337.3 \pm 0.4$  Ma  $-2SD$ , Sláma et al., 2008). In addition, several analyses of the in-house reference zircon BB (Santos et al., 2017) were conducted. BB yielded a concordia age of  $561 \pm 1$  Ma ( $n = 97$ , MSWD = 0.27), which is consistent with the reported ID-TIMS age of this reference material ( $560.0 \pm 0.4$  Ma  $-2SD$ , Santos et al., 2017).

A total of 490 analyses were performed on 312 zircon grains from the four samples; in many cases two analyses were done in different sectors of the same grain that showed different textural and chemical-zoning features in the CL images.

#### 4.2. Zircon Lu–Hf isotope analyses

Following each session of U–Pb isotopic determinations, Lu and Hf isotopic ratios were determined at UFOP, using a Thermo-Fisher Neptune + MC-ICPMS coupled to a Photon Machines 193 ( $\lambda = 193$  nm) ArF Excimer laser ablation system. The 50  $\mu\text{m}$  spot-size laser was fired at 5 Hz repetition rate and  $\sim 3$  J  $\text{cm}^{-2}$  energy

density. Time-resolved profiles of the isotope ratios were processed offline to control the homogeneity of the measured zircons. Corrections for background signal, instrumental mass bias and isobaric interferences of Lu and Yb isotopes on mass 176 were done following the methods by Gerdes and Zeh (2006, 2009). Quoted uncertainties are quadratic additions of the within-run precision and the reproducibility of the reference zircons Temora (Wu et al., 2006), 91500 (Blichert-Toft, 2008), Mud Tank (Woodhead and Hergt, 2005) and BB (Santos et al., 2017). Four reference materials were used before and during runs: Mud Tank, Temora, 91500 and BB. Analyses of the reference zircon Temora yielded an average  $^{176}\text{Hf}/^{177}\text{Hf} = 0.282682 \pm 40$  (2SD,  $n = 33$ ). 41 analyses on the zircon 91500 yielded a  $^{176}\text{Hf}/^{177}\text{Hf} = 0.282317 \pm 70$  (2SD). Mud Tank yielded an average  $^{176}\text{Hf}/^{177}\text{Hf} = 0.282524 \pm 54$  (2SD,  $n = 37$ ). The average  $^{176}\text{Hf}/^{177}\text{Hf}$  for BB was  $0.281676 \pm 62$  (2SD,  $n = 20$ ). These values agree within error with the recommended values for Temora ( $^{176}\text{Hf}/^{177}\text{Hf} = 0.282680 \pm 31$  ( $2\sigma$ ); Wu et al., 2006), 91500 ( $^{176}\text{Hf}/^{177}\text{Hf} = 0.282307 \pm 31$  ( $2\sigma$ ); Blichert-Toft, 2008), Mud Tank ( $^{176}\text{Hf}/^{177}\text{Hf} = 0.282504 \pm 44$  ( $2\sigma$ ); Woodhead and Hergt, 2005) and BB ( $^{176}\text{Hf}/^{177}\text{Hf} = 0.281674 \pm 18$  ( $2\sigma$ ); Santos et al., 2017).

Initial  $^{176}\text{Hf}/^{177}\text{Hf}$  ratios ( $^{176}\text{Hf}/^{177}\text{Hf}_i$ ) were calculated from the measured  $^{176}\text{Lu}/^{177}\text{Hf}$  and  $^{176}\text{Hf}/^{177}\text{Hf}$  ratios using a  $^{176}\text{Lu}$  decay constant of  $\lambda = 1.867 \times 10^{-11} \text{ a}^{-1}$  (Söderlund et al., 2004). Epsilon Hf values and Hf model ages were calculated using Chondritic Uniform Reservoir (CHUR)  $^{176}\text{Lu}/^{177}\text{Hf}$  and  $^{176}\text{Hf}/^{177}\text{Hf}$  ratios of 0.0336 and 0.282785, respectively (Bouvier et al., 2008), Depleted Mantle (DM) values of  $^{176}\text{Lu}/^{177}\text{Hf} = 0.03933$  and  $^{176}\text{Hf}/^{177}\text{Hf} = 0.283294$

(Blichert-Toft and Puchtel, 2010) and an average continental crust composition with a  $^{176}\text{Lu}/^{177}\text{Hf}$  ratio of 0.0113 (Rudnick and Gao, 2003).

Whenever possible, the Lu–Hf laser spot was drilled on top of the U–Pb laser spot. Where this was not the case, care was taken to drill within the same zircon domain (core, rim) previously analysed for U–Pb, characterized by CL imaging. In total, 205 analyses were done on 174 zircon grains.

#### 4.3. Zircon trace element analyses

Trace element concentrations in zircon were analysed using a *Thermo-Fisher Element II* sector field ICP-MS coupled to a *Photon Machines 193 nm ArF Excimer laser* at the Geoscience Department at UFOP. Ablation were performed in a 0.7 L/min He stream using 25  $\mu\text{m}$  laser spot sizes, a repetition rate of 6 Hz and a laser energy density of 10–12  $\text{J cm}^{-2}$ . The He stream was mixed with Ar directly after the ablation cell prior to introduction into the plasma of the ICP-MS. Oxide production, monitored as  $^{254}\text{UO}/^{238}\text{U}$  on the standard glass NIST 612 was well below 1%, and measurements were carried out in low resolution mode, with 15s background and 30s data acquisition. The following isotopes were analysed:  $^{29}\text{Si}$ ,  $^{44}\text{Ca}$ ,  $^{89}\text{Y}$ ,  $^{93}\text{Nb}$ ,  $^{139}\text{La}$ ,  $^{140}\text{Ce}$ ,  $^{141}\text{Pr}$ ,  $^{146}\text{Nd}$ ,  $^{147}\text{Sm}$ ,  $^{153}\text{Eu}$ ,  $^{157}\text{Gd}$ ,  $^{159}\text{Tb}$ ,  $^{163}\text{Dy}$ ,  $^{165}\text{Ho}$ ,  $^{166}\text{Er}$ ,  $^{169}\text{Tm}$ ,  $^{172}\text{Yb}$ ,  $^{175}\text{Lu}$ ,  $^{178}\text{Hf}$ ,  $^{206}\text{Pb}$ ,  $^{208}\text{Pb}$ ,  $^{232}\text{Th}$  and  $^{238}\text{U}$ . Data reduction was performed with GLITTER using  $^{29}\text{Si}$  for internal standardization with  $\text{SiO}_2 = 32.7 \text{ wt.}\%$  for all zircons and the NIST 612 glass as primary standard. The standard glass NIST 610 and basaltic glasses BCR and BHVO-1 have been used as secondary standards. The accuracy of zircon measurements was checked comparing between obtained and recommended concentrations for the standard BCR. This resulted in an offset correction of maximum 10%, which has been applied to the BHVO standard. The corrected results agree for almost all elements (<12% deviation) with recommended values of BHVO and hence, the same correction has been applied to all unknown zircon analyses. Rare earth element (REE) concentrations were normalized to C1 chondrite (McDonough and Sun, 1995).

## 5. Results

### 5.1. Zircon morphology and U–Pb dating

The complete U–Pb data are listed in supplementary data SM-1. Representative zircon CL images, concordia diagrams (calculated using Isoplot/Ex 4; Ludwig, 2003) and Kernel density estimation plots (KDE) and histograms (plotted using DensityPlotter; Vermeesch, 2012) for detrital zircon U–Pb data at the 95% concordance level from each sample are shown in Figs. 3 and 4. The  $^{206}\text{Pb}/^{238}\text{U}$  age was used for zircons <1000 Ma while the  $^{206}\text{Pb}/^{207}\text{Pb}$  age was used for grains older than 1000 Ma. Errors are reported at the  $2\sigma$  level.

Zircons from the garnet-bearing amphibolite sample POC3A and felsic gneiss sample POC3B range in length from 100–400  $\mu\text{m}$ , with length to width ratios from 2:1 to 4:1. Zircons extracted from these two samples are colourless. In CL images, the majority of grains from sample POC3A show euhedral oscillatory-zoned cores, surrounded by weaker luminescence, low contrast rims (Fig. 3a). The rim domains are homogeneous and unzoned or weakly banded. Some detrital cores of the grains are embayed by rims (e.g. grains 13 and 14 in Fig. 3a). In most cases the rims were too small to analyse. However several overgrowths on zircon cores have a larger volume and were analysed (e.g. grains 11–14 in Fig. 3a). A small number of non-prismatic zircon grains show low CL intensity, sector-zonation and no overgrowth (grains 9 and 10 in Fig. 3a). The typical Th/U ratios of euhedral zircon cores range between 0.21 and 0.90, whereas rim overgrowth Th/U ratios are significantly lower

between 0.02 and 0.16 (Table 1 in SM-1). Low CL zircons with sector zoning have either low Th/U ratios of 0.05 (Grain 9 in Fig. 3a) or moderate Th/U of 0.22–0.26 (grain 10 in Fig. 3a). Isotopic data of 114 analyses yielded exclusively Neoproterozoic ages ranging from 560 Ma to 940 Ma (Fig. 4a). The ages of detrital zircon cores cluster around two main peaks at ca. 875 Ma and 800 Ma (Fig. 4a). Sector-zoned grain and rim analyses define a concordia age of  $627.3 \pm 5.3 \text{ Ma}$  (MSWD = 2.0) and this is interpreted as recrystallization age of zircons (Fig. 4a).

Zircons from paragneiss sample POC3B contain euhedral prismatic to anhedral cores with distinct oscillatory zoning (Fig. 3b). Some cores are fractured and contain crosscutting bands (e.g. grains 4, 5, 8, 13 in Fig. 3b). In all grains, cores are surrounded by low CL intensity, homogeneous unzoned rim overgrowths. Similar to sample POC3A some zircons show irregular or sector zoning. The majority of zircon cores have U concentrations below 100 ppm, whereas rims and irregular or unzoned zircons range from 110 to 250 ppm (Table 1 in SM-1). This difference is well reflected in Th/U ratios that differ between cores (0.17–1.22) and rims/irregular and unzoned zircons (<0.10). Results for core and rim analyses are plotted on a concordia diagram and show a similar range in ages as sample POC3A from 610 Ma to 950 Ma (Fig. 4b). The relative probability diagram for detrital cores reveals a main peak at ca. 725 Ma and a less-pronounced peak at ca. 825 Ma (Fig. 4b). Combined rim overgrowth and irregular zoning/unzoned grain analyses define a concordia age of  $628.0 \pm 4.0 \text{ Ma}$  (MSWD = 1.7) interpreted as zircon recrystallization age (Fig. 4b).

Zircon grains extracted from gneiss sample POC28A are prismatic to round in shape and are between 80  $\mu\text{m}$  and 200  $\mu\text{m}$  in length, with length to width ratios of 2:1 to 4:1. CL images show that zircon cores are prismatic and have oscillatory zonation. Cores have sharp contacts to surrounding rim overgrowth that show irregular zoning with different degrees of CL intensity (Fig. 3c). The Th/U ratios of detrital zircon cores range from 0.16 to 2.40 whereas rim overgrowth domains are significantly lower <0.10 (Table 1 in SM-1). The lower Th/U ratios of rims are usually marked by an increase in U concentration. However in some rare cases U concentration of core and rim domains are similar, the low Th/U ratio therefore was caused by an increase in Th concentration. Ages for the paragneiss sample POC28A range from 590 Ma to 2750 Ma. A concordia including all analyses is given in the electronic appendix SM-1 whereas an inset that displays the major age populations is shown in Fig. 4c. A relative probability plot shows that a few detrital zircon cores yielded Meso- to Paleoproterozoic ages with the bulk of the zircons being Neoproterozoic (Fig. 4c). The ages of Neoproterozoic zircons cluster around two main peaks at 680 Ma and 750 Ma and one minor peak at 840 Ma. Rim overgrowth analyses define a concordia age of  $633.0 \pm 3.6 \text{ Ma}$  (MSWD (conc. + equiv.) = 1.8) which is interpreted as recrystallization age (Fig. 4c).

Zircons from the granite sample POC28B range in length from 100 to 250  $\mu\text{m}$ , with length to width ratios from 3:1 to 5:1. Grain shapes are prismatic and CL images reveal oscillatory zonation. Two grains show inherited core and rim overgrowth domain (e.g. grains 9 and 10 in Fig. 3d). The typical range of Th/U ratios is between 0.16 and 1.50 with some exceptions that are below 0.10 or >1.50 (Table 1 in SM-1). The two inherited cores yielded Mesoproterozoic ages with rim overgrowth at ~585 Ma. Excluding the inherited cores, zircons of this sample define a weighted mean  $^{206}\text{Pb}/^{238}\text{U}$  age  $586.6 \pm 3.7 \text{ Ma}$  (MSWD = 10.7) and this is interpreted as the crystallization age of the granitic vein (shown in SM-1).

### 5.2. Lu–Hf isotopes

The Lu–Hf isotope analytical data with concordant U–Pb ages are shown in Table 1 of supplementary material SM-2 and Fig. 5.



**Figure 3.** Representative CL images with U–Pb and Lu–Hf spots of analysed zircons. The U–Pb ages are reported in Ma as  $^{206}\text{Pb}/^{238}\text{U}$  ages for zircons <1000 Ma and  $^{207}\text{Pb}/^{206}\text{Pb}$  ages for zircons >1000 Ma with errors at the  $2\sigma$  level. Calculated  $\epsilon_{\text{Hf}}(t)$  values are given in brackets.

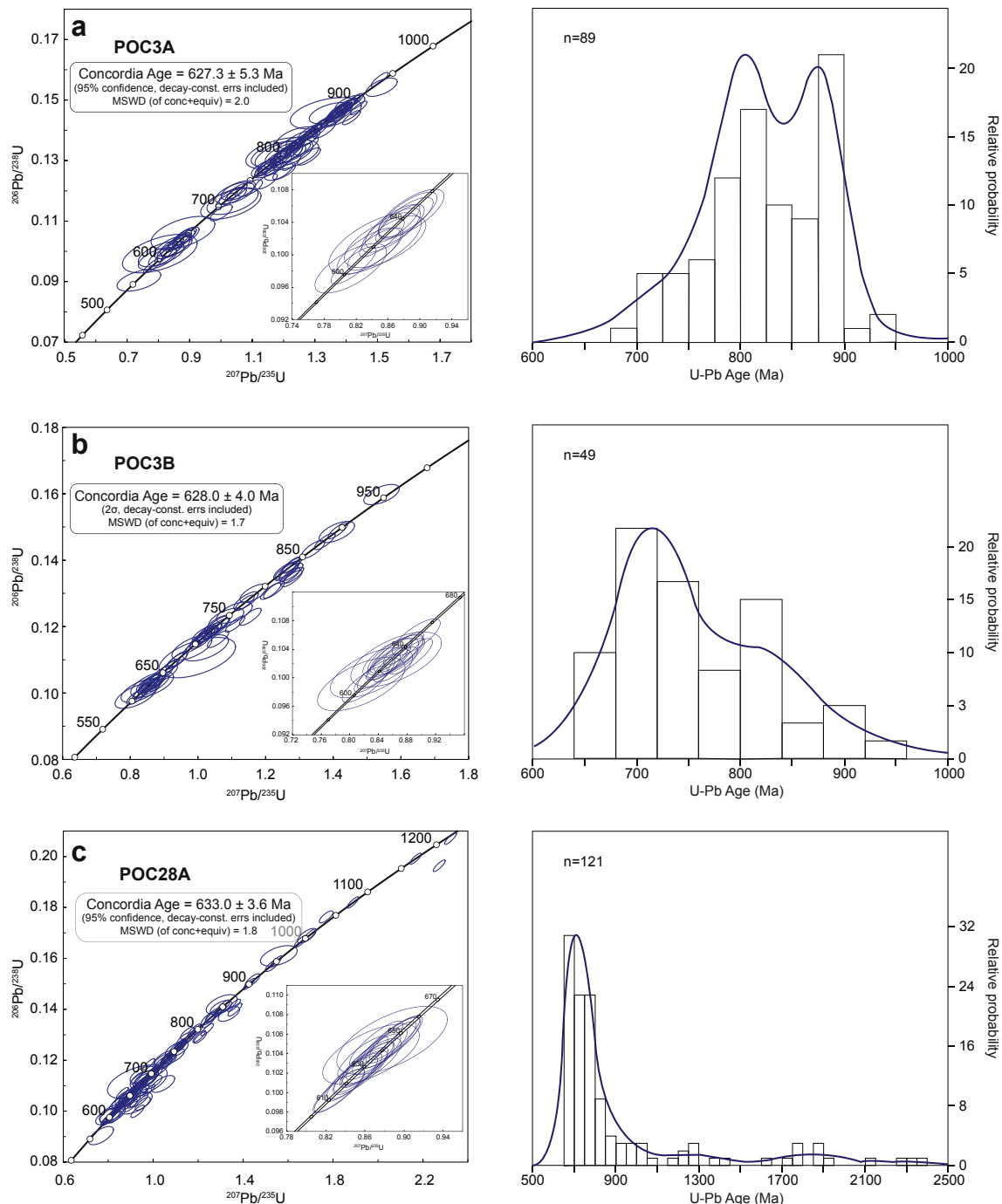


**Figure 4.** Concordia diagrams, Kernel density estimation plots (KDE) and histograms of U–Pb ages plotted for zircons from the Rio Doce Group metasediment samples. The U–Pb ages in KDE plots are reported as  $^{206}\text{Pb}/^{238}\text{U}$  ages for zircons younger than 1000 Ma and as  $^{207}\text{Pb}/^{206}\text{Pb}$  ages for zircons older than 1000 Ma.

Initial  $^{176}\text{Hf}/^{177}\text{Hf}$  of zircon from metasedimentary rocks of the RDG are in the range of 0.28230–0.28288 with superchondritic  $\varepsilon_{\text{Hf}}(t)$  values from  $-1.0$  to 17.9. In contrast, lower  $^{176}\text{Hf}/^{177}\text{Hf}(t)$  were obtained from the intrusion sample with subchondritic  $\varepsilon_{\text{Hf}}(t)$  values. Detailed results for the individual samples are listed below.

Detrital zircon cores from sample POC3A yield  $^{176}\text{Hf}/^{177}\text{Hf}(t)$  from 0.28234 to 0.28255 (Fig. 5a). This corresponds to superchondritic  $\varepsilon_{\text{Hf}}(t)$  values between 2.3 and 11.1. Rim domains yield  $^{176}\text{Hf}/^{177}\text{Hf}(t)$  ratios of 0.28251–0.28265, corresponding to superchondritic  $\varepsilon_{\text{Hf}}(t)$  values ranging from 4.0 to 9.2. Two young zircon grains have lower  $^{176}\text{Hf}/^{177}\text{Hf}(t)$  of 0.28213 that corresponds to a subchondritic  $\varepsilon_{\text{Hf}}(t)$  value of  $-9.6$ .

Slightly higher  $^{176}\text{Hf}/^{177}\text{Hf}(t)$  were obtained from sample POC3B between 0.28242 and 0.28266, corresponding to  $\varepsilon_{\text{Hf}}(t)$  values from 5.1 to 14.9 (Fig. 5b). Zircon overgrowths yield  $^{176}\text{Hf}/^{177}\text{Hf}(t)$  in the range from 0.28251 to 0. This corresponds to superchondritic  $\varepsilon_{\text{Hf}}(t)$  values of 4.4–10.4.

Initial  $^{176}\text{Hf}/^{177}\text{Hf}$  ratios of Neoproterozoic detrital zircons from sample POC28A are in the range of 0.28230–0.28288, corresponding to a range in  $\varepsilon_{\text{Hf}}(t)$  values of  $-1.0$  to 17.9 (Fig. 5c).  $^{176}\text{Hf}/^{177}\text{Hf}(t)$  ratios of zircon rim domains range from 0.28234 to 0.28276, which corresponds to  $\varepsilon_{\text{Hf}}(t)$  values from  $-2.9$  to 13.1. Initial  $^{176}\text{Hf}/^{177}\text{Hf}$  ratios of pre-Neoproterozoic zircons ranges from 0.28108 to 0.28248, which corresponds to  $\varepsilon_{\text{Hf}}(t)$  values of  $-7.5$  to



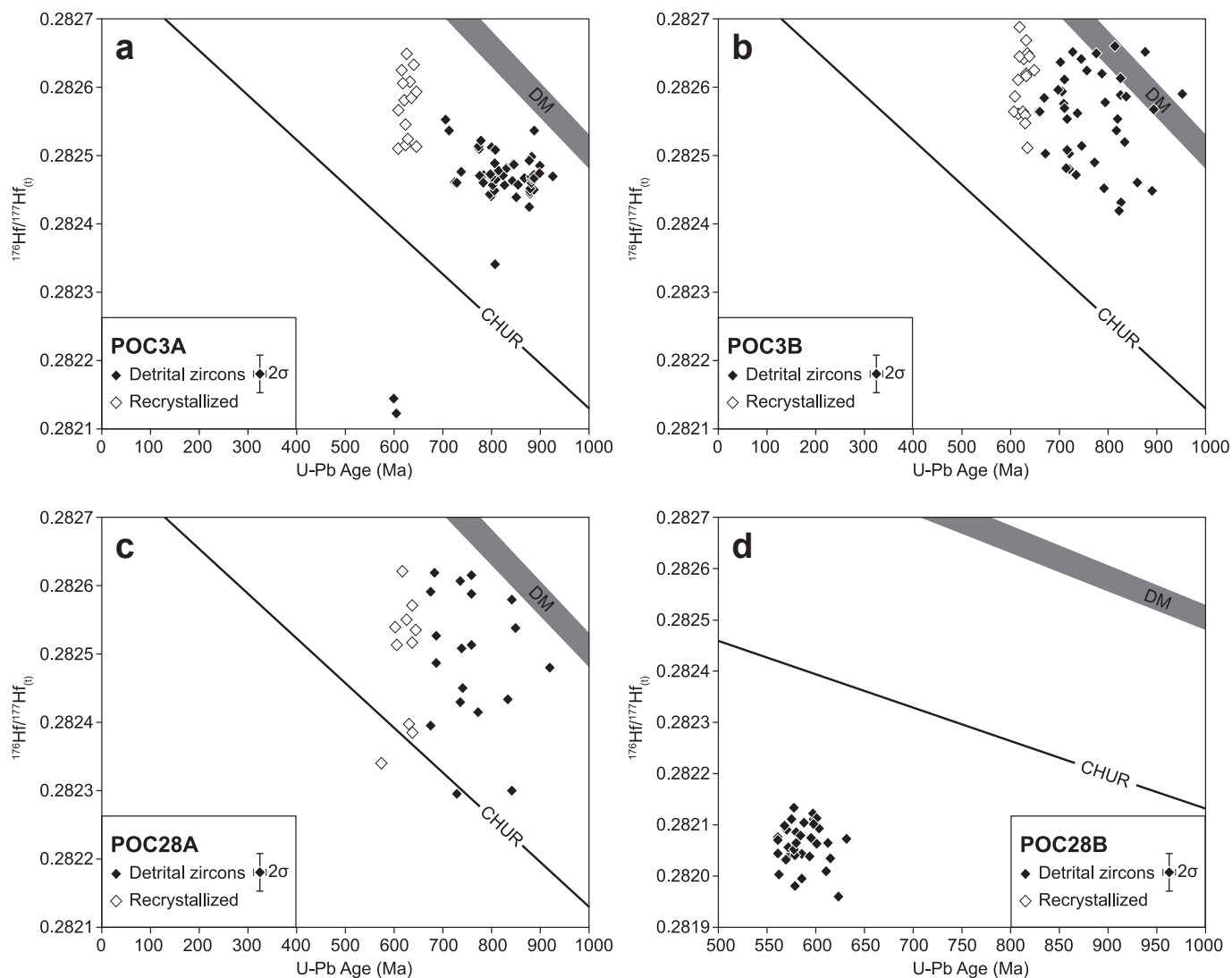


**Figure 5.**  $^{176}\text{Hf}/^{177}\text{Hf}(t)$  vs. U–Pb age diagrams for each sample. Ages are reported as  $^{206}\text{Pb}/^{238}\text{U}$  ages. The Depleted Mantle (DM) field is constructed with compositions from Griffin et al. (2002) and Blichert-Toft and Puchtel (2010).

12.1 (not shown in Fig. 5c). A small number of analyses with anomalously high  $\epsilon_{\text{Hf}}(t)$  values ( $>20$ ) were discarded. The Neoproterozoic zircons of this sample display the same range in  $^{176}\text{Hf}/^{177}\text{Hf}(t)$  and  $\epsilon_{\text{Hf}}(t)$  as samples POC3A and POC3B (Fig. 5).

Excluding two inherited cores, zircons from sample POC28B yield  $^{176}\text{Hf}/^{177}\text{Hf}(t)$  ranging from 0.28196 to 0.28213, with a mean of  $0.28206 \pm 0.00008$  (Fig. 5d), corresponding to subchondritic  $\epsilon_{\text{Hf}}(t)$  values from  $-15.5$  to  $-10.2$ . The inherited cores have initial  $^{176}\text{Hf}/^{177}\text{Hf}$  ratios of 0.28198 and 0.28209, which corresponds to  $\epsilon_{\text{Hf}}(t)$  values of 2.2 and 0.8.

### 5.3. Trace element chemistry

Zircon trace element data are listed in Table 1 of electronic appendix SM-3. Detrital zircon grains have Hf contents of 4000–10,000 ppm, whereas zircons from POC28B range from 5500 to 7500 ppm, and Y contents of 100–2800 ppm and 800–2400 ppm, respectively. Chondrite-normalized REE patterns reveal negative europium anomalies [ $\text{Eu}/\text{Eu} \times \text{N} = 0.07\text{--}1.37$ ; mostly  $<0.4$ ;  $\text{Eu}^* = (\text{Sm} + \text{Gd})_{\text{N}}/2$ ], and positive cerium anomalies [ $\text{Ce}/\text{Ce} \times \text{N} = 0.5\text{--}25$ ; mostly  $<10$ ;  $\text{Ce}^* = (\text{La} + \text{Pr})_{\text{N}}/2$ ] in all

samples. The REE patterns show a variable degree of fractionation as is reflected by  $(\text{Yb}/\text{Sm})_{\text{N}} = 2\text{--}420$  (mostly  $<150$ ) and  $(\text{Yb}/\text{Gd})_{\text{N}} = 1\text{--}170$  (mostly  $<50$ ), whereas the degree of fractionation in sample POC28B is generally lower (Fig. 6). The  $\Sigma\text{REE}$  of analysed zircon grains ranges between 40 ppm and 4000 ppm.

## 6. Discussion

### 6.1. Tectonic depositional environment of the sedimentary rocks

Discrimination diagrams based on whole rock major element compositions are an indication of the tectonic setting and provenance of the RDG sedimentary rocks (Fig. 7). In Roser and Korsch's (1988) discrimination diagram (Fig. 7a), those RDG samples plot in the provenance fields of mafic to intermediate rocks whereas the intrusion sample POC28B plots in the felsic igneous provenance field. Data from the literature plotted for comparison are characterized as sources of felsic igneous or quartzose sedimentary provenance. In Fig. 7b (Bhatia, 1983) the majority of the RDG data plots in the oceanic island arc field with a few samples falling in the island arc and active continental margin field.

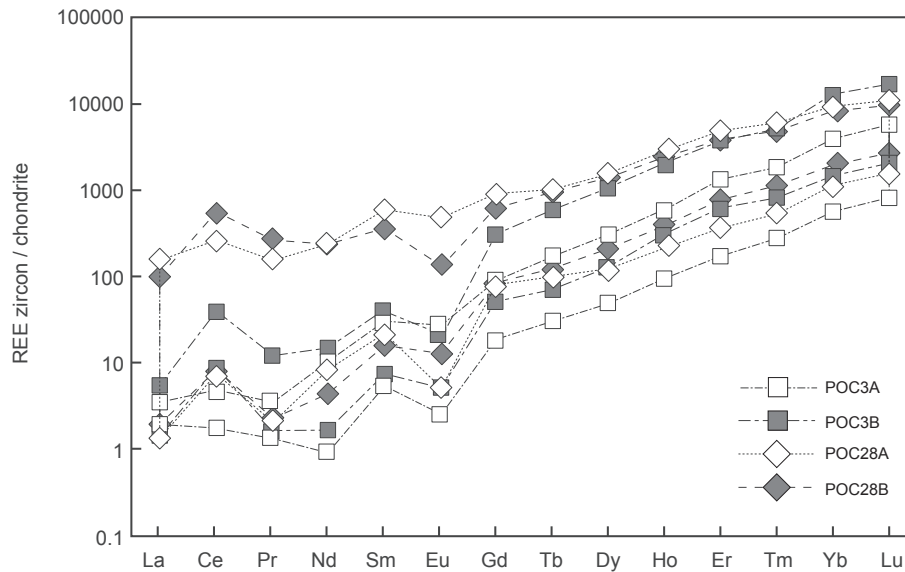


**Figure 6.** Rare earth element (REE) concentrations for detrital zircons normalized to C1 chondrite (McDonough and Sun, 1995).

Discriminant-function-based multi-dimensional diagrams are used in addition to these traditional diagrams of tectonic settings. These additional diagrams enable to discriminate between island/continental arc, continental rift and collision setting of high-silica ( $\text{SiO}_2 = 63\text{--}95$  wt.%; Fig. 7c) and low-silica ( $\text{SiO}_2 = 35\text{--}63$  wt.%; Fig. 7d) rocks (Verma and Armstrong-Altrin, 2013). High-silica samples of the RDG metasedimentary rocks and low-silica sample POC3A plot in the arc tectonic setting whereas low-silica rocks of sample POC28A plots in the rift-setting field.

The trace element chemistry of zircons can be used to fingerprint the provenance of sedimentary rocks by distinguishing between zircons crystallized in either oceanic or continental crust (Grimes et al., 2007). In the U–Yb discrimination diagram zircons of the RDG rocks plot in the oceanic crust provenance field as well as overlapping with the continental crust field (Fig. 8a). The composition of a few zircons of sample POC3A is similar to the field of mafic zircons, which is defined by continental gabbroic rocks (Grimes et al., 2009). In Fig. 8b, the zircon trace element data were plotted in density distribution diagrams based on geochemical proxies for the tectono-magmatic settings of continental arc, ocean island and mid-ocean ridge. Zircons of sample POC3 show a high probability for the ocean island type which is similar to zircons from within-plate/continental rift settings of Rimes et al. (2015). Zircons of sample POC28 plot in the field of continental arc zircons, comparable with zircons from island arc-type ophiolites in the study of Grimes et al. (2015).

Combining the whole-rock data with the zircon trace element dataset it becomes evident that the source of the protoliths of the RDG metasedimentary rocks most likely was mafic to intermediate igneous rocks in an island arc and/or rifting setting. Furthermore our results confirm that the zircon discrimination diagrams by Grimes et al. (2007, 2015) can be applied to detrital zircon populations to distinguish oceanic from continental crust derived zircons.

## 6.2. Age of metamorphism in the RDG

New zircon grows in magmatic or aqueous fluid, or by solid-state formation accompanied by mineral breakdown during metamorphism, whereas existing zircon can be modified by either recrystallization, dissolution-re-precipitation and leaching or Pb

diffusion (e.g. Pidgeon, 1992; Vavra et al., 1996, 1999; Grant et al., 2009). Zircon rims of the RDG metasediments are characterized by low Th/U ratios, irregular shape and homogeneous unzoned habit, which are well-established indicators of zircon recrystallization (e.g. Pidgeon, 1992; Vavra et al., 1999). Large rim overgrowth domains partly truncating euhedral zircon core zonation (Fig. 3) provides evidence for new zircon growth by Ostwald ripening, a viable mechanism for zircon overgrowths formation on larger grains at the expense of smaller zircons in metasedimentary rocks (Vavra et al., 1996; Ayers et al., 2003). Few non-prismatic grains with sector-zoning and low Th/U ratios were found in the RDG metasediments (e.g. grains 9 and 10 in Fig. 3a). The low Th/U ratios and the lack of prismatic face development suggest that these grains formed by recrystallization (Grant et al., 2009).

Several studies have shown that the Hf isotopic composition of zircons is capable of providing further constraints on zircon formation mechanisms during metamorphism (e.g. Zheng et al., 2005; Chen et al., 2010). Zircon rims have similar to slightly higher  $^{176}\text{Hf}/^{177}\text{Hf}_t$  ratios compared to the magmatic cores (Fig. 5). This is consistent with rim overgrowth by recrystallization of pre-existing zircons in a closed system, where breakdown of high  $^{176}\text{Hf}/^{177}\text{Hf}$  ratio phases such as garnet, epidote or monazite had minor influence (e.g. Zheng et al., 2005; Chen et al., 2010). It is therefore concluded that zircon rims of the RDG metasediments formed by recrystallization of existing zircons as well as by consumption of pre-existing smaller grains (Ostwald ripening). Thus, formation of overgrowth domains and sector-zoned zircons is interpreted to result from crystallization during a regional metamorphic event at ca. 630–625 Ma as defined by the concordia ages in Fig. 4.

Syn-collisional metamorphism in the Araçuaí Belt at 575–550 Ma (Richter et al., 2016; Melo et al., 2017) overlaps with orogenic peak metamorphism of the other belts in the Mantiqueira Province from 600 to 560 Ma (Bento dos Santos, 2015 and references therein). In the Ribeira Belt metamorphic overprinting at 620 Ma (Tassinari et al., 2006) marks the onset of collisional metamorphic events, and Silva et al. (1999) reported a gneiss forming event at ~630 Ma. Metamorphic ages of 670–640 Ma in the Ribeira belt were interpreted as a consequence to the formation of a continental magmatic arc (Duffles et al., 2016). A high grade metamorphic event inducing partial melting in the Dom Feliciano Belt was dated at ~650 Ma and related to crustal thickening during

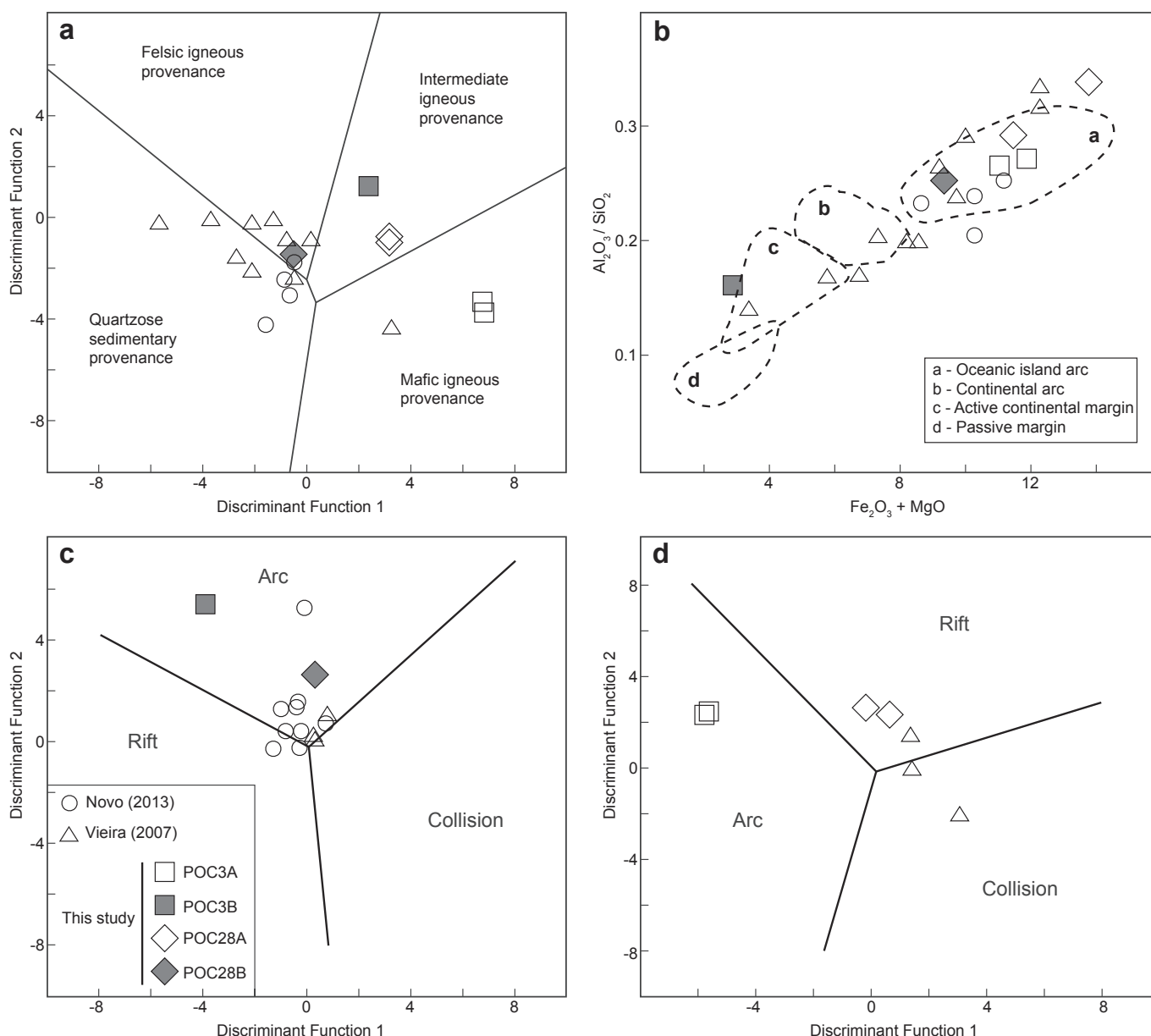


**Figure 7.** Discrimination diagrams for sedimentary rocks: (a) Discriminant-function diagram after Roser and Korsch (1988). (b)  $(\text{Fe}_2\text{O}_3 + \text{MgO})$  (in wt.%) vs.  $\text{Al}_2\text{O}_3/\text{SiO}_2$  diagram (Bhatia, 1983). (c) Discriminant-function diagram for high-silica clastic sediments for three tectonic settings (arc, continental rift, and collision) after Verma and Armstrong-Altrin (2013). (d) Discriminant-function diagram for low-silica clastic sediments for three tectonic settings (arc, continental rift, and collision) after Verma and Armstrong-Altrin (2013). Whole rock data of Rio Doce Group samples from Vieira (2007) and Novo (2013) are shown for comparison. All data are listed in Table 2 of electronic appendix SM-3.

the collision between Rio de la Plata and Congo Cratons (Lenz et al., 2011). The metamorphic event at 630–625 Ma reported for the RDG metasediments in this work is hitherto described in the Araçuaí Belt for the first time. The nature of this event remains, however, a matter for a separate study.

### 6.3. Depositional age constraints on Rio Doce Group metasediments

The three RDG metasediment samples used for detrital zircon U–Pb dating are grouped together for the discussion due to similarity in age spectra and close spatial relationship of outcrops (Fig. 9). The youngest concordant (<5% discordance) magmatic zircon yields an age of  $600 \pm 17$  Ma. This youngest single grain age, however, is separated from a cluster of older detrital zircons with ages of 670–650 Ma. The youngest grain cluster is assumed to be

the more robust measure in this case because the single grain age is analytically not representative for the present dataset of detrital zircons (Dickinson and Gehrels, 2009). We therefore suggest that the youngest zircon among the 670–650 Ma grain cluster represents a realistic maximum depositional age. The deposition of the metasedimentary protolith is then constrained between 650 Ma (maximum depositional age) and 630 Ma (zircon recrystallization event).

### 6.4. Correlation of detrital zircon ages and isotopic data with potential source areas

The U–Pb ages of detrital zircons from the metasedimentary units are shown as probability density plots in comparison to various basins from orogenic belts of the Mantiqueira Province in Fig. 9.

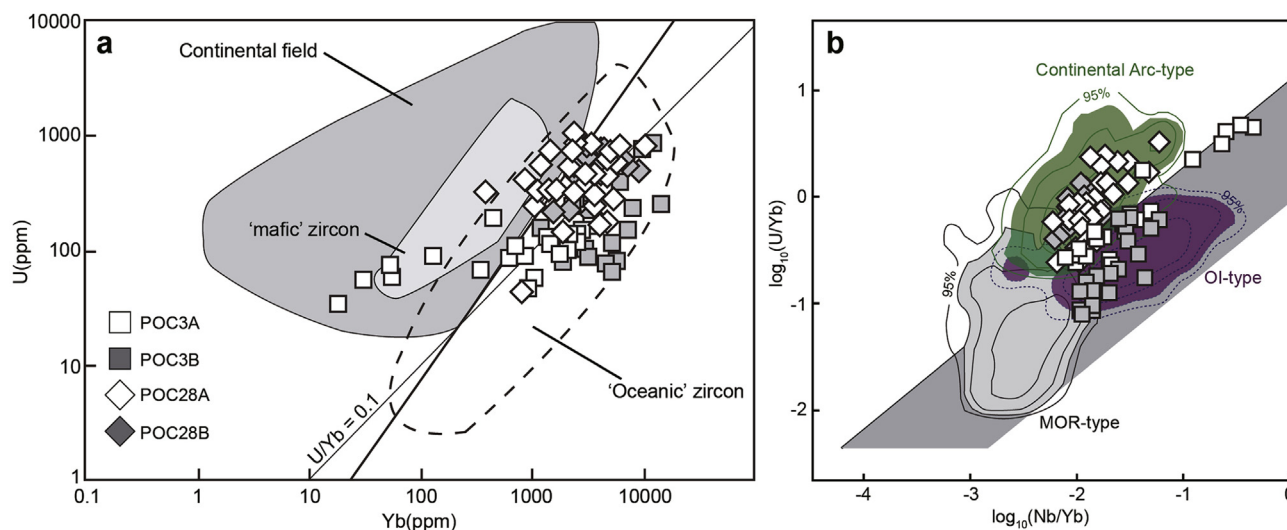


**Figure 8.** (a) U vs. Yb variation diagram with discriminant continental and ocean crust fields from Grimes et al. (2007). (b) Density distribution plots based on geochemical proxies for the tectono-magmatic setting of mid-ocean ridge (MOR-type), plume-influenced ocean-island (OI-type), and continental arc (Cont. arc-type) zircon from Grimes et al. (2015).

A first striking observation is the almost complete restriction of age spectra from RDG metasediments to the Neoproterozoic Era despite the close proximity to Palaeoproterozoic basement rocks. Zircons from outcrop POC3 have Neoproterozoic ages, whereas about 20% of detrital grains from sample POC28A yield small peaks at 2.3, 2.1, 1.8 and 1.3 Ga (Figs. 4 and 9). Potential sources related to these Paleoproterozoic peaks are magmatic and metamorphic complexes in the southern São Francisco Craton region that developed during the Transamazonian Orogeny such as the Mineiro, Mantiqueira, Juiz de Fora or Pocrane Complexes (Alkmim and Marshak, 1998; Noce et al., 2007; Gonçalves et al., 2014). Mesoproterozoic detrital zircons can be linked to rifting events during development of the Espinhaço Supergroup (e.g. Chemale et al., 2012).

The main detrital zircon population within the RDG metasediments ranges from 900 Ma to 650 Ma with subordinate peaks at 875 Ma, 800 Ma and 700 Ma, respectively (Figs. 4 and 9). In the Araçuaí Belt potential sources with zircon growth events are restricted to anorogenic granites of the Salto da Divisa Suite (ca. 875 Ma; Silva et al., 2008) and mafic dykes of the Pedro Lessa Suite (ca. 900 Ma; Machado et al., 1989). The West Congo Belt provides volcanic rocks from the Zadinian and Mayumbian Groups as well as Mativa, Bata Kimenga and Noqui granites as considerable sources (ca. 1000–900 Ma; Tack et al., 2001). Anorogenic alkaline magmatism close to the tectonic contact between the São Francisco Craton and the Araçuaí Belt was dated between 730 Ma and 700 Ma (Rosa et al., 2007) and provides another zircon forming event.

In the following, zircon Hf isotopic data presented here and literature data are used to further constrain source regions. Only the Neoproterozoic detrital zircons are discussed due to their dominant abundance in the age spectra. The  $\epsilon_{\text{Hf}}(t)$  data from RDG samples and available literature data for other belts of the Mantiqueira Province are displayed in Fig. 10. Neoproterozoic zircons of RDG metasedimentary rocks have juvenile signature with  $\epsilon_{\text{Hf}}(t)$  values from 0 to +15 with a distinct cluster between +4 and +14 (Fig. 10) within crustal evolution lines of 1050 Ma and 800 Ma (grey arrows 1 and 2 in Fig. 10). Crustal model ages ( $T_{\text{DM}}$ ) calculated for RDG detrital zircons range between 1.54 Ga and 0.67 Ga with a mean model age of ca. 1 Ga. Suitable source regions need to contain zircons with a juvenile Hf isotopic signature of  $\epsilon_{\text{Hf}}(t)$  between 0 and +15.

We used the terrestrial Hf–Nd array to calculate the corresponding  $\epsilon_{\text{Hf}}(t)$  for given Nd isotope values ( $\epsilon_{\text{Hf}}(t) = 1.36 \times \epsilon_{\text{Nd}}(t)$

+ 2.95; Vervoort et al., 1999) because there is no available Hf isotopic data for potential source areas within the Araçuaí Belt (Salto da Divisa Suite at ca. 875 Ma and mafic dykes of the Pedro Lessa Suite at ca. 900 Ma). Amphibolites of the Araçuaí Belt interpreted as metamorphosed ocean-floor basalts yield crystallization ages at ca. 820 Ma with mantle-like  $\epsilon_{\text{Nd}}(t)$  of 3.4–4.6 (Pedrosa-Soares et al., 1998). Estimated amphibolite bulk rock  $\epsilon_{\text{Hf}}(t)$  of 7.6–9.2 thus fall within the range of RDG metasediment detrital zircons and potentially provided zircons of the ~800 Ma peak. Anorogenic alkaline magmatism north to the Araçuaí Belt shows a mantle-like carbon and oxygen isotopic signature (Rosa et al., 2007).

The Ribeira and Dom Feliciano Belts could be further sources for the 900–650 Ma old zircons. Events associated with zircon growth in the Ribeira Belt are the onset of arc magmatism at ca. 790 Ma (Heilbron and Machado, 2003) and the Rio Negro magmatic arc from 630 Ma to 590 Ma (Tupinambá et al., 2012). The early stage of the Rio Negro Arc of the Ribeira Belt (ca. 790 Ma, 630–620 Ma) has a mantle-like Nd and Sr isotopic composition (Tupinambá et al., 2012).  $\epsilon_{\text{Hf}}(t)$  values estimated from whole rock Nd isotopic data from –1.1 to +9.8 overlaps with the Hf isotopic composition of detrital zircons from the RDG metasediments. However, there is a lack of zircon grains between 790 Ma and 630 Ma and a continued development of the magmatic arc is an assumption (Heilbron and Machado, 2003; Tupinambá et al., 2012). Some zircon data (Degler et al., 2017) from metasedimentary rocks in the Araçuaí Belt show significant overlap in age and Hf isotope composition with RDG zircons (Fig. 10). These authors considered the Rio Negro Arc the source of the zircons.

The São Gabriel terrane within the Dom Feliciano Belt provides a model for possible sources with ophiolites and intra-oceanic magmatic arc sequences around 900–680 Ma (e.g. Babinski et al., 1996; Lena et al., 2014; Arena et al., 2016). Oceanic crust formation in the DFB dated between 750 Ma and 700 Ma included zircon with positive  $\epsilon_{\text{Nd}}(t)$  values and model ages from 1000 Ma to 800 Ma (Babinski et al., 1996). These model ages fit with the calculated Hf  $T_{\text{DM}}$  ages of 1.5–0.7 Ga of the RDG detrital zircons. Additionally estimated  $\epsilon_{\text{Hf}}(t)$  of +6.8 to +13.6 overlap with the  $\epsilon_{\text{Hf}}(t)$  values of detrital zircons from the studied metasediments. This is further corroborated by ophiolitic sequences within the São Gabriel terrane with zircon  $\epsilon_{\text{Hf}}(t)$  values from +1 to +15 and Hf model ages of  $T_{\text{DM}} = 1.3–0.7$  Ga (Arena et al., 2016, 2017a, b; Fig. 10). Hence,

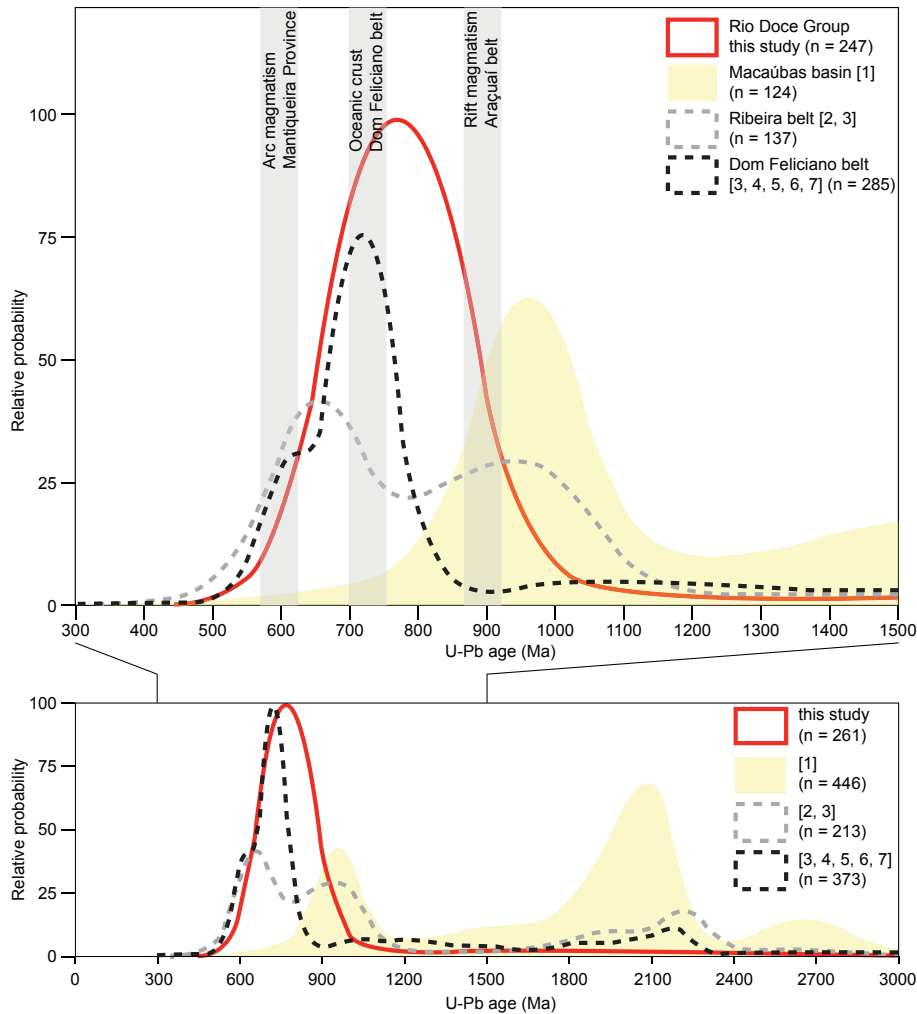


**Figure 9.** Detrital zircon age spectra of the Rio Doce Group metasediment samples plotted versus detrital age spectra of other basins and units from the Araçuaí, Ribeira and Dom Feliciano Belts. Data compiled from Basei et al. (2005, 2008, 2011), Lena et al. (2014), Fernandes et al. (2015), Kuchenbecker et al. (2015), and Pertille et al. (2015). Diagrams were constructed using *DensityPlotter* (Vermeesch, 2012).

erosion of rocks similar to the São Gabriel terrane of the DFB could have provided zircons to the protolith of the RDG metasediments due to their correspondence in age and Hf isotopic composition.

Many studies successfully linked detrital zircon age spectra with zircon forming events in potential source areas. The reconstruction of the palaeogeographic link between sources and sediments further constrain the tectonic evolution of geological terranes (e.g. Augustsson et al., 2006; Cawood et al., 2007; Howard et al., 2009). The protoliths of the RDG metasediments were derived from erosion of rift-related magmatic rocks, ophiolites and/or intra-oceanic magmatic arcs within the Mantiqueira Province. This interpretation is based on the similarity between detrital zircon ages in the RDG metasediments and intervals of zircon growth events in the Araçuaí Belt and adjacent belts of the Brasiliano/Pan-African Orogeny. The contribution of rift-related rocks from the West Congo Belt is considered as minor because only a small cluster of detrital zircons of the RDG metasediments range in age from 1000 Ma to 900 Ma.

This correspondence of variable sources is further substantiated by isotopic constraints. However in many instances either the isotopic dataset is insufficient to clarify potential source regions or estimations are made of available whole rock Nd isotopic data. Potentially any of the presented rift-related zircon forming events could have provided detrital inputs into the RDG metasediment

protoliths, since they all show juvenile mantle-like signatures. Notwithstanding the best correspondence in age and zircon Hf isotope and trace element composition is found for oceanic crustal rocks of the Dom Feliciano Belt. Similar rock associations in the Araçuaí Belt may have sourced the zircons.

#### 6.5. Comparison with existing detrital zircon data and tectonic setting of the protoliths

In addition to potential zircon growth events, the detrital zircon age and isotopic data of the RDG metasediments are compared to other detrital zircon data from the Mantiqueira Province (Figs. 9–11). To visualize this comparison, a compilation of zircon-forming magmatic events and the detrital zircon record of basins in the Mantiqueira Province during the Neoproterozoic are shown in the light of rifting events in Fig. 11.

The Macaúbas Basin is interpreted to be the precursor basin of the Araçuaí and West Congo Orogeny recording a major glacial event and the evolution from a rift setting to a gulf basin (Pedrosa-Soares et al., 2001; Babinski et al., 2012; Kuchenbecker et al., 2015). Detrital zircon spectra of the Macaúbas Group show prominent peaks at ca. 2.0 Ga and 1.0 Ga with some Mesoproterozoic and Archean contributions (Fig. 9; Babinski et al., 2012; Kuchenbecker et al., 2015). These peaks are attributed to reworked basement of

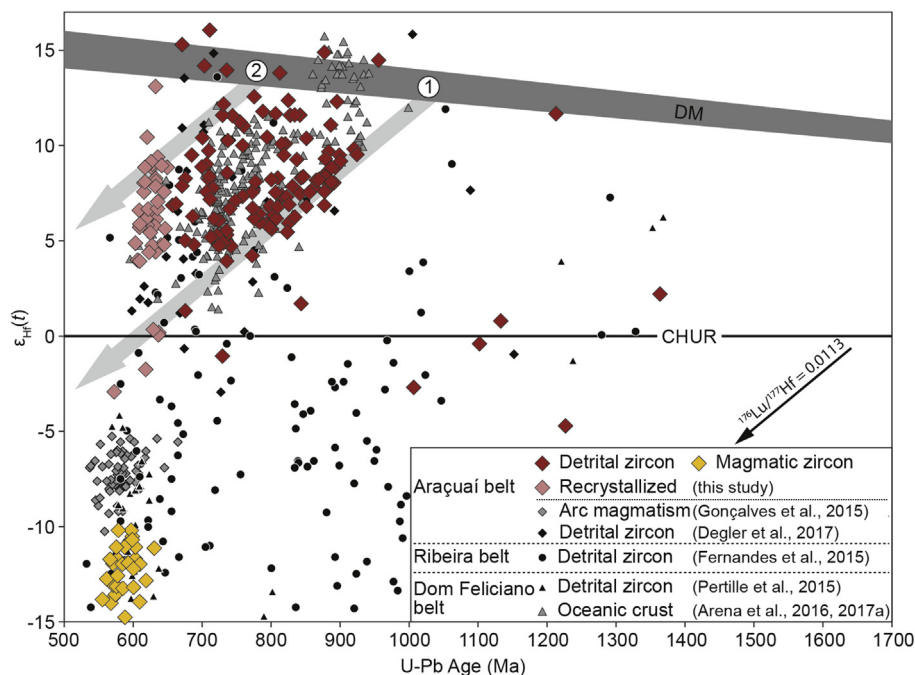


**Figure 10.**  $\epsilon_{\text{Hf}}(t)$  vs. age diagram for detrital and recrystallized zircons from this study. The diagonal grey arrows indicate crustal evolution trends at 1050 Ma (1) and 800 Ma (2) using an average  $^{176}\text{Lu}/^{177}\text{Hf}$  of 0.0113 for the average continental crust (Rudnick and Gao, 2003). The crustal evolution arrays fit through the  $\epsilon_{\text{Hf}}(t)$  compositions of detrital zircons from this study. Data of detrital zircons, arc magmatism and oceanic crust formation from other orogenic belts of west Gondwana are plotted for comparison. The Depleted Mantle (DM) evolution is as in Fig. 5.

the São Francisco and Congo Cratons during the Transamazonian Orogeny as well as the rifting event at around 1000–900 Ma of the Congo Craton (Tack et al., 2001). Zircons of the earlier rift stage <900 Ma however are very scarce compared to the RDG metasedimentary rocks (Figs. 9 and 11). The difference in detrital zircon age spectra between the Macaúbas Basin and the RDG metasediments suggests that the protoliths to the RDG metasediments were deposited in a different basin system, further away from reworked basement rocks and closer to rift-related magmatism.

Detrital zircons from the Ribeira Belt display a major peak around 750–600 Ma and a smaller peak at ca. 1050–850 Ma with minor peaks in the Paleoproterozoic and Archean (Fig. 9; Fernandes et al., 2015). Detrital zircon from the Neoproterozoic Búzios succession show positive zircon  $\epsilon_{\text{Hf}}(t)$  values of 0 to +13 and  $T_{\text{DM}}$  of 1.5–1.0 Ga (Fernandes et al., 2015). This unit was interpreted to be a back-arc basin or an intra-oceanic realm deposited in an extensional setting. A convergent system as source for zircons with juvenile Hf isotopic composition is ruled out due to the gap of continental arc magmatism between 790 Ma and 630 Ma (Fig. 11; Fernandes et al., 2015).

The Porongos Group of the DFB displays detrital zircon populations at 800–650 Ma, a broad cluster between 1500–1050 Ma and a minor peak at 2200 Ma with  $\epsilon_{\text{Hf}}(t)$  values of –18 to –4 (Figs. 9–11; Pertille et al., 2015, 2017). Its tectonic setting is described as a cordilleran foreland basin with detrital zircon contribution from reworked crust (Pertille et al., 2015). Hence it shows no correspondence with the RDG metasedimentary rocks. Detrital zircons from metasedimentary units within the São Gabriel terrane range in age from 840 Ma to 660 Ma with a pronounced peak around 750–700 Ma (Fig. 9; Lena et al., 2014). The O isotopic composition of these zircons is indicative of mantle-derived magmatism with progressive assimilation of altered crust (Lena et al., 2014). Lena et al. (2014) proposed a progressive tectonic setting from intra-oceanic arc to a continental active margin for metasediments of the São Gabriel terrane.

Considering the correspondence of detrital zircon ages and isotopic composition between the RDG metasediments and metasediments from the Buzios succession and São Gabriel terrane, we suggest that the protoliths to the RDG metasediments were deposited in a similar tectonic setting. Scarcity in Mesoproterozoic to Archean detrital zircons indicates distance to the continental margin. Thus, we propose an intra-oceanic arc setting for the deposition of the protoliths to the RDG metasediments, which agrees with the results of whole rock and zircon trace element discrimination diagrams. The detrital zircon age spectra of the studied samples fit well with those suggested by Cawood et al. (2012) for back-arc basins.

Richter et al. (2016) recently studied the Nova Venécia Complex (NVC), which is supposedly a back-arc basin related to the pre-collisional magmatic arc of the Araçuaí Belt. Their work shows detrital zircon ages ranging from 900 Ma to 700 Ma, similar to the RDG metasediments (Fig. 11). However, detrital zircons dated at 650–610 Ma indicate proximity to the continental magmatic arc in comparison to the RDG metasediments (Fig. 11). Another difference is the record of metamorphic events at ~570 Ma and ~540 Ma (Richter et al., 2016). Therefore the protoliths to the metasediments of the NVC and RDG initially shared a similar source for detrital zircons but subsequently underwent a different tectonic evolution.

#### 6.6. Tectonic evolution and geodynamic implications

The RDG metasediments are characterized by a geological history that is different from neighbouring units: (1) the juvenile signature and zircon age spectra show that the metasediments are distinct from the adjacent Paleoproterozoic basement at their western boundary and hence are not their reworked products; (2) zircons of the RDG metasediments record a different metamorphic event from paragneiss units of the NVC to their eastern boundary; (3) they are unrelated to pre-collisional magmatism because no ages near 630–580 Ma are recorded; (4) boundaries to adjacent

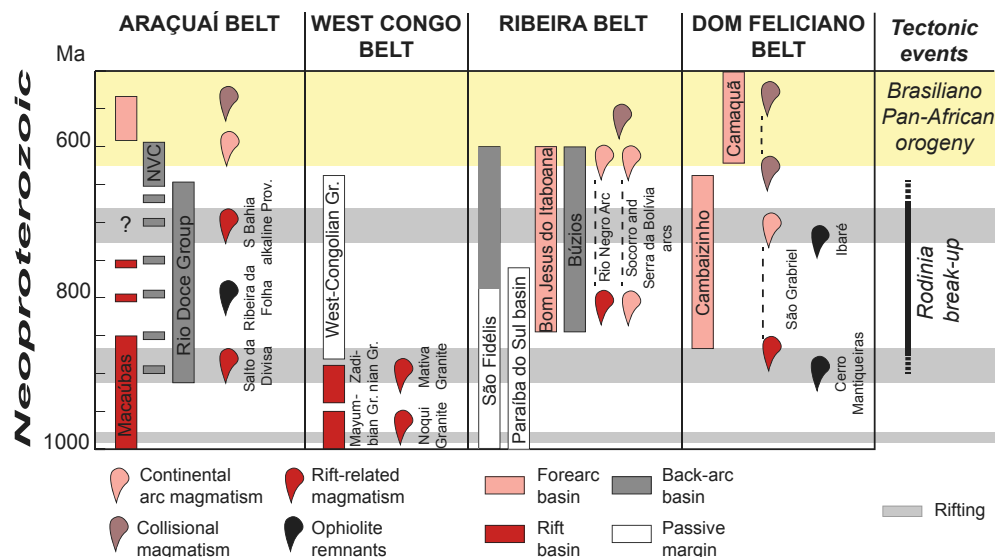


**Figure 11.** Stratigraphic correlation chart for Neoproterozoic magmatic events and basins adjacent to orogenic belts of the Mantiqueira Province. Ages of sedimentary basins are based on actual detrital zircon abundances (see text for explanation and references).

units are defined by thrust and transcurrent faults. It is therefore concluded that the RDG metasediments represent an allochthonous terrane.

The origin of the 650–900 Ma old zircons with positive  $\varepsilon_{\text{Hf}}(t)$  in the protoliths of the RDG metasediments may be correlated to rift-related magmatism in the Araçuai Belt (Rosa et al., 2007; Silva et al., 2008) and possibly also to juvenile arcs and oceanic crust formation in the Ribeira and Dom Feliciano Belts (Babinski et al., 1996; Tupinambá et al., 2012; Lena et al., 2014; Arena et al., 2016). The pattern of age spectra from the RDG metasediments is suggestive of a back-arc basin setting (Cawood et al., 2012) whereas the paucity of pre-Neoproterozoic detrital zircons points to deposition of protoliths sediments distal to the continents and in proximity to the source. However the arc cannot be represented by pre-collisional magmatism in the Araçuai Belt considering the differences in zircon ages and Hf isotopic composition. We interpret that detrital zircons of the protoliths of the RDG metasediments were sourced from oceanic crust consistent with ophiolite remnants in the Araçuai Belt at ca. 800 Ma (Pedrosa-Soares et al., 1998) and intra-oceanic magmatic arcs. Tectonic setting discrimination diagrams (Figs. 7 and 8) and Fig. 11 further constrain that the protoliths to the RDG metasediments were deposited in an oceanic island-arc setting. Contribution of detrital input from the Ribeira and Dom Feliciano Belt (Fernandes et al., 2015; Arena et al., 2016) is not ruled out. We concur with previous studies (Pedrosa-Soares et al., 2001; Alkmim et al., 2006) that a mantle plume-related rifting event led to the opening of an oceanic basin, and that the onset of this rifting stage was at ca. 900 Ma as evidenced by a first cluster of detrital zircons of the RDG (Figs. 4 and 11). A strong mantle contribution is indicated by positive  $\varepsilon_{\text{Hf}}(t)$  values of detrital zircons from the RDG metasediments as well as positive  $\varepsilon_{\text{Nd}}(t)$  values from oceanic crust remnants (Pedrosa-Soares et al., 1998). The protoliths were deposited as pelites with compositional variations, which were transformed to felsic gneisses and amphibolites during metamorphism. Juvenile magmatism is recorded in the detrital zircon record until 650 Ma. This maximum depositional age is interpreted as the transition from an extensional to a convergent setting.

The second stage involves subduction of the newly formed oceanic plate beneath an upper plate represented by the Paleoproterozoic basement. Sedimentary bodies, including the protoliths to the RDG metasediments, and fragments of thicker crustal bodies

are scraped off the subducting oceanic crust and accreted to the upper plate. Related ophiolite bodies are further evidence of an accretionary process. Terrane accretion can cause regional metamorphism in a scenario such as proposed here (e.g. Hudson and Plafker, 1982; Monger et al., 1982). Therefore the zircon recrystallization recorded at ca. 630 Ma in RDG metasediments might be due to a regional metamorphic event during accretion. Similar metamorphic ages have been described in Degler et al. (2017).

In a final stage ongoing subduction of oceanic crust led to partial melting to produce the pre-collisional magmatism that intruded the RDG metasediments. Zircons of the pre-collisional magmatism display Hf isotopic compositions with  $\varepsilon_{\text{Hf}}(t)$  of  $-15$  to  $-10$  and Hf model ages of 1.9–2.2 Ga (Fig. 7; Gonçalves et al., 2015). These results argue for reworking of the Paleoproterozoic basement to account for the continental arc magma production. The intrusion at ca. 585 Ma (sample POC28B) did, however, not affect zircons from the RDG metasediments.

The results presented in this study have implications for the palaeogeographic reconstruction of West Gondwana. Zircons of the RDG metasediments provide evidence for zircon growth events related to juvenile magmatism in a range from ca. 900–650 Ma. This sets a time frame for the final break-up of the São Francisco–Congo Cratons in the northern section of the Mantiqueira Province. Furthermore, the juvenile character of the RDG metasediments and zircon trace element data suggest the existence of an island arc in a precursor basin to the Araçuai Belt. Zircons of several units in the Ribeira and Dom Feliciano Belts to the south are similar in age and Hf isotopic composition with the RDG (Fig. 12a). Additionally, zircon trace element compositions overlap with those of ophiolite-derived zircons from the Dom Feliciano Belt (Fig. 12b). The similarity in ages for juvenile magmatism and oceanic basin settings in the Ribeira and Dom Feliciano Belts are consistent with a large connected oceanic system. The combined evolution of the Araçuai and Ribeira Belts is rarely addressed but has been suggested elsewhere (Richter et al., 2016; Degler et al., 2017). Here we propose that the rifting and break-up of the entire orogenic system prior to Gondwana amalgamation was connected even farther to the south including the Dom Feliciano Belt (Fig. 12).

The break-up of supercontinents is often related to mantle plumes or superplumes (e.g. Li et al., 2003; Ernst et al., 2013; Murphy and Nance, 2013) whereas they are not necessarily the

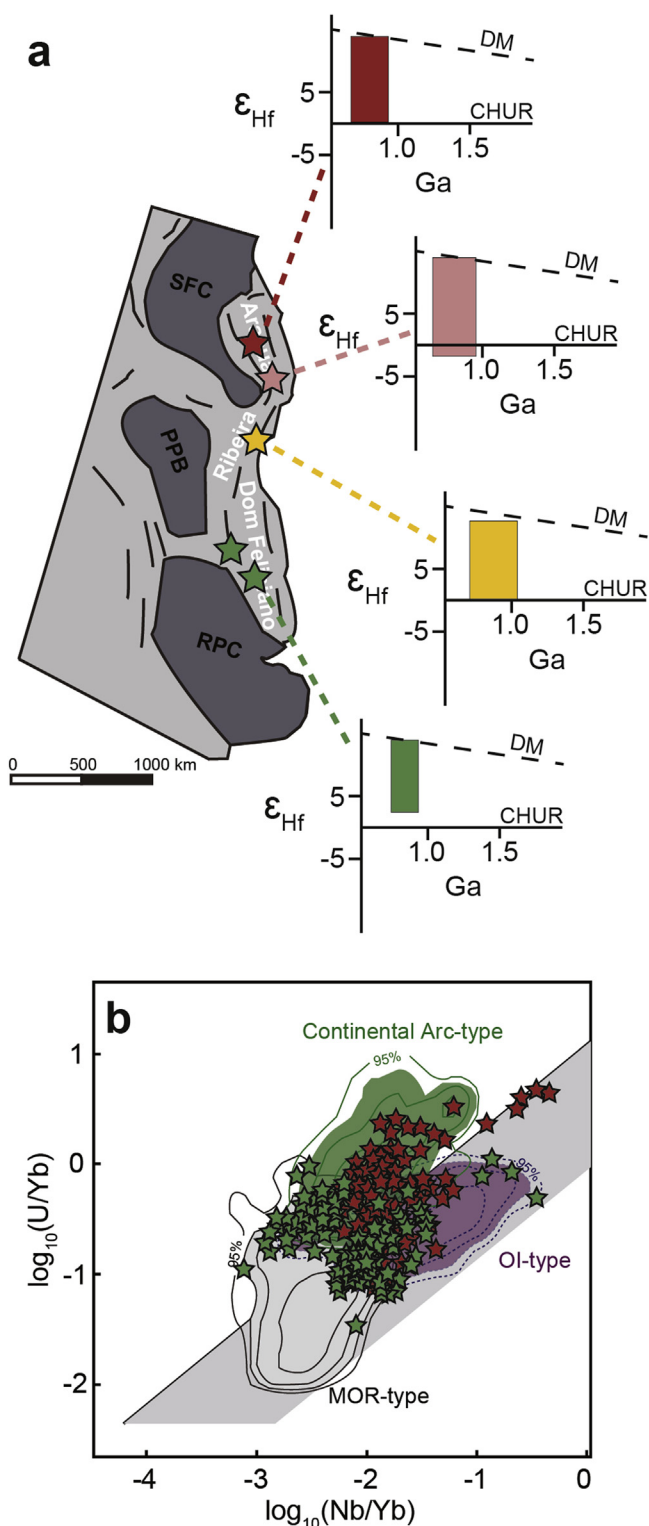


**Figure 12.** Sketch illustrating the similarity in zircon age and composition of selected units in the Mantiqueira Province: (a) Simplified  $\epsilon_{\text{Hf}}(t)$  vs. age diagrams corresponding to samples of the different orogenic belts with data from Fernandes et al. (2015), Arena et al. (2016, 2017a) and Degler et al. (2017). (b) Tectonic setting discrimination diagram (Grimes et al., 2015) with data from Arena et al. (2017a, b).

main driving force (Cawood et al., 2016). However, the synchronicity of juvenile rift-related magmatism in the entire Mantiqueira Province is suggestive for a large plume that evoked break-up of its proto-continents. It further implicates that the cratonic blocks

involved in the Mantiqueira Province (Congo–São Francisco, Rio de la Plata and Kalahari) most likely were connected as early as ~900 Ma. Subsequently these blocks underwent a similar geodynamic evolution until final West Gondwana assembly.

## 7. Conclusions

Detrital zircons of metasedimentary rocks from the Rio Doce Group in the Araçuaí Belt of SE Brazil, the northern orogenic sector of the Mantiqueira Province, have been studied in order to constrain their provenance. The conclusions of this U–Pb–Hf isotope and trace element work and their broader implications can be summarized as follows:

- (1) The protoliths to the metasediments were deposited in an ocean or intra-oceanic arc basin distal to the continent with a maximum depositional age of ca. 650 Ma. Detrital zircons are nearly exclusively Neoproterozoic in age displaying a major population from 650–900 Ma with strongly positive  $\epsilon_{\text{Hf}}(t)$  values. The potential source rocks are represented by rift-related magmatism and oceanic crust formation in the Araçuaí Belt. Further potential contributions from juvenile arcs and oceanic crust assemblages of the Ribeira and Dom Feliciano Belts to the south are possible.
- (2) Transition to convergence lead to accretion of the terrane that included the RDG metasediments to the Paleoproterozoic basement. An accretion-related regional metamorphic event invokes zircon recrystallization at ca. 630 Ma. Subsequently this terrane is intruded by pre-collisional magmatism at ca. 585 Ma, which did not affect the zircons of the RDG metasediments.
- (3) Correlation in age and zircon Hf isotopic and trace element composition from the entire Mantiqueira Province suggests that a mantle plume caused synchronous rift-related magmatism evidencing the onset of final break-up of the São Francisco–Congo Craton and adjacent cratonic blocks at around 900 Ma with a peak at ca. 750 Ma. This further implies that the involved cratonic blocks (Congo–São Francisco, Rio de la Plata and Kalahari) were connected as early as 900 Ma irrespective of their position within Rodinia.
- (4) The simultaneity of rifting in all orogenic belts of the Mantiqueira Province is consistent with a synchronous geodynamic evolution during the Brasiliano–Pan-African Orogeny.

## Acknowledgements

The authors wish to acknowledge funding from CNPq (401334/2012-0–302058/2015-0–402852/2012-5) and FAPEMIG (APQ03943–RPQ-0067-10–RDP00063-10) grants. We thank Ana Alkmim for assistance with analytical work. Comments by two anonymous reviewers and editorial handling by Wenjiao Xiao improved the manuscript.

## Appendix A. Supplementary data

Supplementary data related to this article can be found at <https://doi.org/10.1016/j.gsf.2018.02.011>.

## References

- Alkmim, F.F., Marshak, S., 1998. Transamazonian Orogeny in the Southern São Francisco Craton Region, Minas Gerais, Brazil: Evidence for Paleoproterozoic collision and collapse in the Quadrilátero Ferrífero. *Precambrian Research* 90, 29–58.
- Alkmim, F.F., Marshak, S., Pedrosa-Soares, A.C., Peres, G.G., Cruz, S.C., Whittington, A., 2006. Kinematic evolution of the araçuaí–west Congo orogen in Brazil and Africa: nutcracker tectonics during the neoproterozoic assembly of Gondwana. *Precambrian Research* 149, 43–63.



- Almeida, F.F.M., Hasui, Y., Brito-Neves, B.B., Fuck, R.A., 1981. Brazilian structural provinces: an introduction. *Earth Science Reviews* 17, 1–29.
- Andersen, T., 2005. Detrital zircons as tracers of sedimentary provenance: limiting conditions from statistics and numerical simulation. *Chemical Geology* 216, 249–270.
- Arena, K.R., Hartmann, L.A., Lana, C., 2016. Evolution of Neoproterozoic ophiolites from the southern Brasiliano Orogen revealed by zircon U–Pb–Hf isotopes and geochemistry. *Precambrian Research* 285, 299–314.
- Arena, K.R., Hartmann, L.A., Lana, C., 2017a. Tonian emplacement of ophiolites in the southern Brasiliano Orogen delimited by U–Pb–Hf isotopes of zircon from metasediments. *Gondwana Research* 49, 296–332.
- Arena, K.R., Hartmann, L.A., Lana, C., 2017b. U–Pb–Hf isotopes and trace elements of metamorphic zircon delimit the evolution of neoproterozoic Capané ophiolite in the southern Brasiliano Orogen. *International Geology Review*. <https://doi.org/10.1080/00206814.2017.1355269> (in press).
- Augustsson, C., Münker, C., Bahlburg, H., Fanning, C.M., 2006. Provenance of late Palaeozoic metasediments of the SW South American Gondwana margin: a combined U–Pb and Hf-isotope study of single detrital zircons. *Journal of Geological Society London* 163, 983–995.
- Ayers, J.C., de la Cruz, K.J., Miller, C.F., Switzer, O., 2003. Experimental study of zircon coarsening in quartzite±H<sub>2</sub>O at 1.0 GPa and 1000 °C, with implications for geochronological studies of high-grade metamorphism. *American Mineralogist* 88, 365–376.
- Babinski, M., Achemale Jr., F., Hartmann, L.A., Van Schmus, W.R., Silva, L.C., 1996. Juvenile accretion at 750–700 Ma in southern Brazil. *Geology* 24, 439–442.
- Babinski, M., Pedrosa-Soares, A.C., Trindade, R.I.F., Martins, M., Noce, C.M., Liu, D., 2012. Neoproterozoic glacial deposits from the Araçuaí orogen, Brazil: age, provenance and correlations with the São Francisco craton and West Congo belt. *Gondwana Research* 21, 451–465.
- Basei, M.A.S., Frimmel, H.E., Nutman, A.P., Preciozzi, F., Jacob, J., 2005. A connection between the Neoproterozoic Dom Feliciano (Brazil/Uruguay) and Gariép (Namibia/South Africa) orogenic belts – evidence from a reconnaissance provenance study. *Precambrian Research* 139, 195–221.
- Basei, M.A.S., Frimmel, H.E., Nutman, A.P., Preciozzi, F., 2008. West Gondwana amalgamation based on detrital zircon ages from Neoproterozoic Ribeira and Dom Feliciano belts of South America and comparison with coeval sequences from SW Africa. *Journal of Geological Society of London* 294, 239–256.
- Basei, M.A.S., Campos Neto, M.C., Castro, N.A., Nutman, A.P., Wemmer, M.T., Yamamoto, M.T., Hueck, M., Osako, L., Siga Jr., O., Passareli, C.R., 2011. Tectonic evolution of the brusque group, Dom Feliciano belt, Santa Catarina. *Journal of South American Earth Sciences* 32, 324–350.
- Bento dos Santos, T.M., Tassinari, C.C.G., Fonseca, P.E., 2015. Diachronic collision, slab break-off and long-term high thermal flux in the Brasiliano–Pan-African orogeny: implications for the geodynamic evolution of the Mantiqueira Province. *Precambrian Research* 260, 1–22.
- Bhatia, M.R., 1983. Plate tectonics and geochemical composition of sandstones. *The Journal of Geology* 91, 611–627.
- Blichert-Toft, J., 2008. The Hf isotopic composition of zircon reference material 91500. *Chemical Geology* 253, 252–257.
- Blichert-Toft, J., Puchtel, I.S., 2010. Depleted mantle sources through time: evidence from Lu–Hf and Sm–Nd isotope systematics of Archean komatiites. *Earth and Planetary Science Letters* 297, 598–606.
- Bouvier, A., Vervoort, J.D., Patchett, P.J., 2008. The Lu–Hf and Sm–Nd isotopic composition of CHUR: constraints from unequilibrated chondrites and implications for the bulk composition of terrestrial planets. *Earth and Planetary Science Letters* 273, 48–57.
- Brito-Neves, B.B., Cordani, U., 1991. Tectonic evolution of south America during the late proterozoic. *Precambrian Research* 53, 23–40.
- Brito-Neves, B.B., Campos Neto, M.C., Fuck, R.A., 1999. From Rodinia to western Gondwana: an approach to the Brasiliano–Pan African cycle and orogenic collage. *Episodes* 22, 155–166.
- Campos Neto, M.C., Figueiredo, M.C.H., 1995. The Rio Doce orogeny, southeastern Brazil. *Journal of South American Earth Sciences* 8, 143–162.
- Cawood, P.A., Nemchin, A.A., Strachan, R., 2007. Provenance record of Laurentian passive-margin strata in the northern Caledonides: implications for paleo-drainage and paleogeography. *The Geological Society of America Bulletin* 119, 993–1003.
- Cawood, P.A., Hawkesworth, C.J., Dhuime, B., 2012. Detrital zircon record and tectonic setting. *Geology* 40, 875–878.
- Cawood, P.A., Stachan, R.A., Pisarevsky, S.A., Gladkochub, D.P., Murphy, J.B., 2016. Linking collisional and accretionary orogens during Rodinia assembly and breakup: implications for models of supercontinent cycles. *Earth and Planetary Science Letters* 449, 118–126.
- Chemale, F., Dussin, I.A., Alkmim, F.F., Martins, M.S., Queiroga, G., Armstrong, R., Santos, M.N., 2012. Unravelling a Proterozoic basin history through detrital zircon geochronology: the case of the Espinhaço Supergroup, Minas Gerais, Brazil. *Gondwana Research* 22, 200–206.
- Chen, R.X., Zheng, Y.F., Xie, L.W., 2010. Metamorphic growth and recrystallization of zircon: distinction by simultaneous in-situ analyses of trace elements, U–Th–Pb and Lu–Hf isotopes in zircons from eclogite-facies rocks in the Sulu orogen. *Lithos* 114, 132–154.
- D'Agrella-Filho, M.S., Cordani, U.G., 2017. The paleomagnetic record of the São Francisco-Congo Craton. In: Heilbron, M., et al. (Eds.), *São Francisco Craton, Eastern Brazil*, *Regional Geology Reviews*, pp. 305–320.
- Degler, R., Pedrosa-Soares, A., Dussin, I., Queiroga, G., Schulz, B., 2017. Contrasting provenance and timing of metamorphism from paragneisses of the Araçuaí–Ribeira orogenic system, Brazil: Hints for Western Gondwana assembly. *Gondwana Research* 51, 30–50.
- Dickinson, W.R., Gehrels, G.E., 2009. Use of U–Pb ages of detrital zircons to infer maximum depositional ages of strata: a test against a Colorado Plateau Mesozoic database. *Earth and Planetary Science Letters* 288, 115–125.
- Duffles, P., Trouw, R.A.J., Mendes, J.C., Gerdes, A., Vinagre, R., 2016. U–Pb age of detrital zircon from the Embu sequence, Ribeira belt, SE Brazil. *Precambrian Research* 278, 69–86.
- Ernst, R.E., Bleeker, W., Söderlund, U., Kerr, A.C., 2013. Large Igneous Provinces and supercontinents: toward completing the plate tectonic revolution. *Lithos* 174, 1–14.
- Evans, D.A.D., 2009. The palaeomagnetically viable, long-lived and all-inclusive Rodinia supercontinent reconstruction. *Geological Society London Special Publications* 327, 371–404.
- Evans, D.A.D., Trindade, R.I.F., Catelani, E.L., D'Agrella-Filho, M.S., Heaman, L.M., Oliveira, E.P., Söderlund, U., Ernst, R.E., Smirnov, A.V., Salminen, J.M., 2016. Return to Rodinia? Moderate to high palaeolatitude of the São Francisco/Congo craton at 920 Ma. *Geological Society London Special Publications* 424, 167–190.
- Fernandes, G.L.F., Schmitt, R.S., Bongiolo, E.M., Basei, M.A.S., Mendes, J.C., 2015. Unraveling the tectonic evolution of a Neoproterozoic–Cambrian active margin in the Ribeira Orogen (SE Brazil): U–Pb and Lu–Hf provenance data. *Precambrian Research* 266, 337–360.
- Frimmel, H.E., Basei, M.S., Gaucher, C., 2011. Neoproterozoic geodynamic evolution of SW-Gondwana: a southern African perspective. *International Journal of Earth Sciences* 100, 323–354.
- Grant, M.L., Wilde, S.A., Wu, F., Yang, J., 2009. The application of zircon cathodoluminescence imaging, Th–U–Pb chemistry and U–Pb ages in interpreting discrete magmatic and high-grade metamorphic events in the North China Craton at the Archean/Proterozoic boundary. *Chemical Geology* 261, 155–171.
- Gehrels, G., 2014. Detrital zircon U–Pb geochronology applied to tectonics. *Annual Review of Earth and Planetary Science Letters* 42, 127–149.
- Gerdes, A., Zeh, A., 2006. Combined U–Pb and Hf isotope LA–(MC)–ICP–MS analyses of detrital zircons: comparison with SHRIMP and new constraints for the provenance and age of an Armorican metasediment in Central Germany. *Earth and Planetary Science Letters* 249, 47–61.
- Gerdes, A., Zeh, A., 2009. Zircon formation versus zircon alteration – new insights from combined U–Pb and Lu–Hf in-situ LA–ICP–MS analyses, and consequences for the interpretation of Archean zircon from the Central Zone of the Limpopo Belt. *Chemical Geology* 261, 230–243.
- Gonçalves, L., Farina, F., Lana, C., Pedrosa-Soares, A.C., Alkmim, F., Nalini Jr., H.A., 2014. New U–Pb ages and lithochemical attributes of the Ediacaran Rio Doce magmatic arc, Araçuaí confined orogen, southeastern Brazil. *Journal of South American Earth Sciences* 52, 129–148.
- Gonçalves, L., Alkmim, F.F., Pedrosa-Soares, A.C., Dussin, I.A., Valeriano, C.M., 2015. Granites of the intracontinental termination of a magmatic arc: an example from the Ediacaran Araçuaí orogen, southeastern Brazil. *Gondwana Research* 36, 439–458.
- Griffin, W.L., Wang, X., Jackson, S.E., Pearson, N.J., O'Reilly, S.Y., Xu, X., Zhou, X., 2002. Zircon chemistry and magma mixing, SE China: in-situ analysis of Hf isotopes, Tonglu and Pingtan igneous complexes. *Lithos* 61, 237–269.
- Grimes, C.B., John, B.E., Kelemen, P.B., Mazdab, F., Wooden, J.L., Cheadle, M.J., Hanghøj, K., Schwartz, J.J., 2007. The trace element chemistry of zircons from oceanic crust: a method for distinguishing detrital zircon provenance. *Geology* 35, 643–646.
- Grimes, C.B., John, B.E., Cheadle, M.J., Mazdab, F.K., Wooden, J.L., Swapp, S., Schwartz, J.J., 2009. On the occurrence, trace element geochemistry, and crystallization history of zircon from in situ ocean lithosphere. *Contributions to Mineralogy and Petrology* 158, 757–783.
- Grimes, C.B., Wooden, J.L., Cheadle, M.J., John, B.E., 2015. “Fingerprinting” tectonomagmatic provenance using trace elements in igneous zircon. *Contributions to Mineralogy and Petrology* 170, 46.
- Heilbron, M., Machado, N., 2003. Timing of terrane accretion in the neoproterozoic–eopalaeozoic Ribeira orogen SE Brazil. *Precambrian Research* 125, 87–112.
- Hoffman, P.F., Kaufman, A.J., Halverson, G.P., Schrag, D.P., 1998. A neoproterozoic snow-ball earth. *Science* 281, 1342–1346.
- Howard, K.E., Hand, M., Barovich, K.M., Reid, A., Wade, B.P., Belousova, E.A., 2009. Detrital zircon ages: improving interpretation via Nd and Hf isotopic data. *Chemical Geology* 262, 277–292.
- Hudson, T., Plafker, G., 1982. Paleogene metamorphism of an accretionary flysch terrane, eastern Gulf of Alaska. *The Geological Society of America Bulletin* 93, 1280–1290.
- Jackson, S.E., Pearson, N.J., Griffin, W.L., Belousova, E.A., 2004. The application of laser ablation-inductively coupled plasma-mass spectrometry to in situ U–Pb zircon geochronology. *Chemical Geology* 211, 47–69.
- Kuchenbecker, M., Pedrosa-Soares, A.C., Babinski, M., Fanning, M., 2015. Detrital zircon age patterns and provenance assessment for pre-glacial to post-glacial successions of the Neoproterozoic Macaúbas Group, Araçuaí orogen, Brazil. *Precambrian Research* 266, 12–26.
- Leite, J.A.D., Hartmann, L.A., Fernandes, L.A.D., Mc Naughton, N.J., Soliani Jr., E., Koester, E., Santos, J.O.S., Vasconcelos, M.A.Z., 2000. Zircon U–Pb SHRIMP dating of gneissic basement of the Dom Feliciano Belt, southernmost Brazil. *Journal of South American Earth Sciences* 13, 739–750.
- Lena, L.O.F., Pimentel, M.M., Philipp, R.P., Armstrong, R., Sato, K., 2014. The evolution of the Neoproterozoic São Gabriel juvenile terrane, southern Brazil based on high spatial resolution U–Pb ages and  $\delta^{18}\text{O}$  data from detrital zircons. *Precambrian Research* 247, 126–138.

- Lenz, C., Fernandes, L.A.D., McNaughton, N.J., Porcher, C.C., Masquelin, H., 2011. U–Pb SHRIMP ages for the cerro bori orthogneisses, Dom Feliciano belt in Uruguay: evidences of a ~800 Ma magmatic and ~650 Ma metamorphic event. *Precambrian Research* 185, 149–163.
- Li, Z.X., Li, X.H., Kinny, P.D., Wang, J., Zhang, S., Zhou, H., 2003. Geochronology of Neoproterozoic syn-rift magmatism in the Yangtze Craton, South China and correlations with other continents: evidence for a mantle superplume that broke up Rodinia. *Precambrian Research* 122, 85–109.
- Li, Z.X., Bogdanova, S.V., Collins, A.S., Davidson, A., De Waele, B., Ernst, R.E., Fitzsimons, I.C.W., Fuck, R.A., Gladkochub, D.P., Jacobs, J., Karlstrom, K.E., Lu, S., Natapov, L.M., Pease, V., Pisarevsky, S.A., Thrane, K., Vernikovsky, V., 2008. Assembly, configuration, and break-up history of Rodinia: a synthesis. *Precambrian Research* 160, 179–210.
- Ludwig, K.R., 2003. Isoplot/Ex Version 3.00: a Geochronological Toolkit for Microsoft Excel. Berkeley Geochronology Center, Berkeley, CA.
- Machado, N., Schrank, A., Abreu, F.R., Knauer, L.G., Abreu, P.A.A., 1989. Resultados preliminares da geocronologia U–Pb na serra do Espinhaço Meridional. *Boletim Socioeconomico Brasileira de Geologia Núcleo MG* 10, 171–174.
- McDonough, W.F., Sun, S.S., 1995. The composition of the Earth. *Chemical Geology* 120, 223–253.
- Meert, J.G., Lieberman, B.S., 2008. The neoproterozoic assembly of Gondwana and its relationship to the ediacaran–Cambrian radiation. *Gondwana Research* 14, 5–21.
- Melo, M.G., Stevens, G., Lana, C., Pedrosa-Soares, A.C., Frei, D., Alkmim, F.F., Alkmim, L.A., 2017. Two cryptic anatectic events within a syn-collisional granulite from the Araçuaí orogen (southeastern Brazil): evidence from the polymetamorphic Carlos Chagas batholith. *Lithos* 277, 51–71.
- Monger, J.W.H., Price, R.A., Tempelman Kluit, D.J., 1982. Tectonic accretion and the origin of the two major metamorphic and plutonic belts in the Canadian Cordillera. *Geology* 10, 70–75.
- Murphy, J.B., Nance, R.D., 2013. Speculations on the mechanisms for the formation and breakup of supercontinents. *Geoscience Frontiers* 4, 185–194.
- Nance, R.D., Murphy, J.B., Santosh, M., 2014. The supercontinent cycle: a retrospective essay. *Gondwana Research* 25, 4–29.
- Noce, C., Pedrosa-Soares, A.C., Silva, L., Armstrong, R., Piuzeana, D., 2007. Evolution of polycyclic basement complexes in the Araçuaí Orogen based on U–Pb SHRIMP data: implications for Brazil–Africa links in Paleoproterozoic time. *Precambrian Research* 159, 60–78.
- Novo, T.A., 2013. Caracterização do Complexo Pocrane, magmatismo básico mesoproterozóico e unidades neoproterozóicas do sistema Araçuaí–Ribeira, com ênfase em geocronologia U–Pb (SHRIMP e LA-ICP-MS). Universidade Federal de Minas Gerais. Belo Horizonte 193.
- Oriolo, S., Oyhantçabal, P., Wemmer, K., Siegesmund, S., 2017. Contemporaneous assembly of Western Gondwana and final Rodinia break-up: implications for the supercontinent cycle. *Geoscience Frontiers* 8, 1431–1445.
- Pedrosa-Soares, A.C., Vidal, F., Leonardos, O.H., Brito-Neves, B.B., 1998. Neoproterozoic oceanic remnants in eastern Brazil: further evidence and refutation of an exclusively ensialic evolution for the Araçuaí–West Congo Orogen. *Geology* 26, 519–522.
- Pedrosa-Soares, A.C., Noce, C.M., Wiedmann, C.M., Pinto, C.P., 2001. The Araçuaí–West-Congo Orogen in Brazil: an overview of a confined orogen formed during Gondwanaland assembly. *Precambrian Research* 110, 307–323.
- Pedrosa-Soares, A.C., Campos, C.P., Noce, C.M., Silva, L.C., Novo, T.A., Roncato, J., Medeiros, S., Castañeda, C., Queiroga, G.N., Dantas, E., Dussin, I.A., Alkmim, F.F., 2011. Late neoproterozoic–Cambrian granitic magmatism in the Araçuaí orogen (Brazil), the eastern Brazilian pegmatite province and related mineral resources. *Journal of Geological Society London* 350, 25–51.
- Pertille, J., Hartmann, L.A., Philipp, R.P., Petry, T.S., Lana, C., 2015. Origin of the ediacaran Porongos group, Dom Feliciano belt, southern Brazilian shield, with emphasis on whole rock and detrital zircon geochemistry and U–Pb, Lu–Hf isotopes. *Journal of South American Earth Sciences* 64, 69–93.
- Pertille, J., Hartmann, L.A., Santos, J.O.S., McNaughton, N.J., Armstrong, R., 2017. Reconstructing the Cryogenian–Ediacaran evolution of the Porongos fold and thrust belt, Southern Brazilian Orogen, based on Zircon U–Pb–Hf–O isotopes. *International Geology Review* 59, 1532–1560.
- Pidgeon, R.T., 1992. Recrystallization of oscillatory zoned zircon: some geochemical and petrological implications. *Contributions to Mineralogy and Petrology* 110, 463–472.
- Rapela, C.W., Fanning, C.M., Casquet, C., Pankhurst, R.J., Spalletti, L., Poiré, D., Baldo, E.G., 2011. The Rio de la Plata craton and the adjoining Pan-African/Brazilian terranes: their origins and incorporation into south-west Gondwana. *Gondwana Research* 20, 673–690.
- Richter, F., Lana, C., Stevens, G., Buick, I., Pedrosa-Soares, A.C., Alkmim, F.F., Cutts, K., 2016. Sedimentation, metamorphism and granite generation in a back-arc region: records from the ediacaran Nova Venécia Complex (Araçuaí orogen, southeastern Brazil). *Precambrian Research* 272, 78–100.
- Rosa, M.L.S., Conceição, H., Macambira, M.J., Galarza, M.A., Cunha, M.P., Menezes, R.C.L., Marinho, M.M., Cruz-Filho, B.E., Rios, D.C., 2007. Neoproterozoic anorogenic magmatism in the Southern Bahia Alkaline Province of NE Brazil: U–Pb and Pb–Pb ages of the blue sodalite syenites. *Lithos* 97, 88–97.
- Roser, B.P., Korsch, R.J., 1988. Provenance signatures of sandstone mudstone suites determined using discriminant function analysis of major element data. *Chemical Geology* 67, 119–139.
- Rudnick, R.L., Gao, S., 2003. Composition of the continental crust. In: Rudnick, R.L. (Ed.), *Treatise on Geochemistry*. Elsevier-Perigamon, Oxford, pp. 1–64.
- Saalmann, K., Hartmann, L.A., Remus, M.V.D., Koester, E., Conceição, R.V., 2005. Sm–Nd isotope geochemistry of metamorphic volcano-sedimentary successions in the São Gabriel belt, southernmost Brazil: evidence for the existence of juvenile Neoproterozoic oceanic crust to the east of the La Plata Craton. *Precambrian Research* 136, 159–175.
- Santos, M.M., Lana, C., Scholz, R., Buick, I., Schmitz, M.D., Kamo, S.L., Gerdes, A., Corfu, F., Tapster, S., Lancaster, P., Storey, C.D., Basei, M.A.S., Tohver, E., Alkmim, A., Nalini, H., Krambrock, K., Fantini, C., Wiedenbeck, M., 2017. A new appraisal of Sri Lankan BB zircon as a reference material for LA-ICP-MS U–Pb geochronology and Lu–Hf isotope tracing. *Geostandards and Geoanalytical Research*. <https://doi.org/10.1111/ggr.12167>.
- Silva, L.C., Hartmann, L.A., McNaughton, N.J., Fletcher, I.R., 1999. Shrimp U–Pb zircon dating of Neoproterozoic granitic magmatism and collision in the Pelotas Batholith, southernmost Brazil. *International Geology Review* 41, 531–551.
- Silva, L.C., McNaughton, N.J., Armstrong, R., Hartmann, L., Fletcher, I., 2005. The Neoproterozoic Mantiqueira Province and its African connections: a zircon-based U–Pb geochronological subdivision for the Brasiliano/Pan-African systems of orogens. *Precambrian Research* 136, 203–240.
- Silva, L.C., Soares, A.C.P., Texeira, L.R., Armstrong, R., 2008. Tonian rift-related, A-type continental plutonism in the Araçuaí Orogen, eastern Brazil: new evidence for the breakup stage of the São Francisco–Congo Palecontinent. *Gondwana Research* 13, 527–537.
- Sláma, J., Kosler, J., Condon, D.J., Crowley, J.L., Gerdes, A., Hanchar, J.M., Horstwood, M.S.A., Morris, G.A., Nasdala, L., Norberg, N., Schaltegger, U., Schoene, B., Tubrett, M.N., Whitehouse, M.J., 2008. Plešovice zircon – a new natural reference material for U–Pb and Hf isotopic microanalysis. *Chemical Geology* 249, 1–35.
- Söderlund, U., Patchett, J.P., Vervoort, J.D., Isachsen, C.E., 2004. The <sup>176</sup>Lu decay constant determined by Lu–Hf and U–Pb isotope systematics of Precambrian mafic intrusions. *Earth and Planetary Science Letters* 219, 311–324.
- Stacey, J.S., Kramers, J.D., 1975. Approximation of terrestrial lead isotope evolution by a two-stage model. *Earth and Planetary Science Letters* 26, 207–221.
- Tack, L., Wingate, M.T.D., Liégeois, J.-P., Fernandez-Alonso, M., Deblond, A., 2001. Early neoproterozoic magmatism (1000–910Ma) of the zadinian and mayumbian groups (bas–Congo): onset of Rodinian rifting at the western edge of the Congo craton. *Precambrian Research* 110, 277–306.
- Tassinari, C.C.G., Munhá, J.M.U., Dias Neto, C.M., Bento dos Santos, T., Cordani, U.G., Nutmann, A., Fonseca, P.E., 2006. In: Constraints on the thermochronological evolution of Ribeira fold belt, SE Brazil: evidence for long-term elevated geothermal gradient of neoproterozoic orogenies. Abstracts of the V South American Symposium on Isotope Geology, Punta del Este, pp. 200–203.
- Trompette, R., 1997. Neoproterozoic (~600 Ma) aggregation of western Gondwana: a tentative scenario. *Precambrian Research* 82, 101–112.
- Tuller, M., 2000. Projeto leste-MG. Folha ipanema (SE.24-Y-C-IV), belo horizonte, SEME/COMIG/CPRM. Escala 1, 100.000.
- Tupinambá, M., Heilbron, M., Valeriano, C.M., Porto Jr., R., Dios, F.B., Machado, N., Almeida, J.C.H., 2012. Juvenile contribution of the neoproterozoic Rio Negro magmatic arc (Ribeira belt, Brazil): implications for western Gondwana amalgamation. *Gondwana Research* 21, 422–438.
- Van Acherbergh, E., Ryan, C.G., Jackson, S.E., Griffin, W., 2001. Data reduction software for LA-ICP-MS. In: Sylvester, P. (Ed.), *Laser Ablation ICPMS in the Earth Sciences*, 29. Mineralogical Association of Canada, pp. 239–243.
- Vavra, G., Gebauer, D., Schmid, R., Compston, W., 1996. Multiple zircon growth and recrystallization during polyphase Late Carboniferous to Triassic metamorphism in granulites of the Ivrea Zone (Southern Alps): an ion microprobe (SHRIMP) study. *Contributions to Mineralogy and Petrology* 122, 337–358.
- Vavra, G., Schmid, R., Gebauer, D., 1999. Internal morphology, habit and U–Th–Pb microanalysis of amphibolite-to-granulite facies zircons: geochronology of the Ivrea Zone (Southern Alps). *Contributions to Mineralogy and Petrology* 134, 380–404.
- Verma, S.P., Armstrong-Altrin, J.S., 2013. New multi-dimensional diagrams for tectonic discrimination of siliciclastic sediments and their application to Precambrian basins. *Chemical Geology* 355, 117–133.
- Vermeesch, P., 2012. On the visualization of detrital age distributions. *Chemical Geology* 312–313, 190–194.
- Vervoort, J.D., Patchett, P.J., Blichert-Toft, J., Albaredo, F., 1999. Relationships between Lu–Hf and Sm–Nd isotopic systems in the global sedimentary system. *Earth and Planetary Science Letters* 168, 79–99.
- Vieira, V.S., 2007. Significado do Grupo Rio Doce no Contexto do Orógeno Araçuaí. Belo Horizonte (Ph.D. thesis). Universidade Federal de Minas Gerais.
- Woodhead, J.D., Hergt, J.M., 2005. A preliminary appraisal of seven natural zircon reference materials for in situ Hf isotope determination. *Geostandards and Geoanalytical Research* 29, 183–195.
- Wu, F.Y., Yang, Y.H., Xie, L.W., Yang, J.H., Xu, P., 2006. Hf isotopic compositions of the standard zircons and baddeleyites used in U–Pb geochronology. *Chemical Geology* 234, 105–126.
- Zheng, Y.F., Wu, Y.B., Zhao, Z.F., Zhang, S.B., Xu, P., Wu, F.Y., 2005. Metamorphic effect on zircon Lu–Hf and U–Pb isotope systems in ultrahigh-pressure eclogite-facies metagranite and metabasite. *Earth and Planetary Science Letters* 240, 378–400.